*International Journal of Remote Sensing*, March 2010



Taylor & Francis

**Review Article**

# A current review of empirical procedures of remote sensing in inland and near-coastal transitional waters

MARK WILLIAM MATTHEWS[*]†

† Marine Remote Sensing Unit, Department of Oceanography, University of Cape Town, South Africa

The empirical approach of remote sensing has a proven capability to provide timely and accurate information on inland and near-coastal transitional waters. This paper gives a thorough review of empirical algorithms for quantitatively estimating a variety of parameters from spaceborne, airborne and *in situ* remote sensors in inland and transitional waters, including: chlorophyll *a* (Chl *a*), total suspended solids (TSS), Secchi disk depth ($z_{SD}$), turbidity, absorption by coloured dissolved organic matter ($a_{CDOM}$), and other parameters e.g. phycocyanin (PC). Current remote sensing instruments are also reviewed. The theoretical basis of the empirical algorithms is given using fundamental bio-optical theory of the inherent optical properties (IOPs). Bands, band ratios and band arithmetic algorithms that could be used to produce common biogeophysical products for inland/transitional waters are identified. The paper discusses the potential role that empirical algorithms could play alongside more advanced model-based algorithms in the future of water remote sensing, especially for near real-time operational monitoring systems. The paper aims to describe the current status of empirical remote sensing in inland and near-coastal transitional waters and provide a useful reference to workers. It does not cover 'inversion' algorithms.

## 1. Introduction.

The recent launch of many new satellite instruments, and advances in computer technologies, has greatly increased the range of successful water-related remote sensing applications, and improved real-time monitoring of water quality and the rapid detection of environmental threats such as eutrophication and HABs (Mertes 2002, Ritchie *et al.* 2003, Glasgow *et al.* 2004, Power *et al.* 2005). Remote sensing offers substantial advantages over traditional monitoring methods, mainly because of the synoptic coverage and temporal consistency of the data, and has the potential to provide crucial information on inland and near-coastal transitional waters in countries where conventional water quality monitoring programmes are either lacking or unsatisfactory (Navalgund *et al.* 2007). The great number of recent publications on the remote detection of a variety of biogeophysical parameters in inland and near-coastal transitional waters is testament to the rapidly growing interest in the subject (Table 1). These waters are often optically complex and commonly known as 'Case 2' (Morel and Prieur 1977) being a function of at least three optically-active constituents (phytoplankton, CDOM and *tripton*) which may vary independently of one another. Therefore these waters have more demanding requirements for instrument spectral resolution and sensitivity, atmospheric correction accuracy, and water constituent retrieval algorithms (IOCCG 2000). Parameters often derived quantitatively using empirical

[*]Corresponding author. Email address: Mark.matthews@uct.ac.za

methods from remotely sensed data include phytoplankton pigments such as Chl *a* (Gitelson *et al.* 2009), cyanobacterial pigment phycocyanin (PC) (Ruiz-Verdú *et al.* 2008), concentration of Total Suspended Solids (TSS) (Doxaran *et al.* 2009), absorption by Coloured Dissolved Organic Matter ($a_{CDOM}$) (Kutser *et al.* 2005a), Secchi disk depth ($z_{SD}$) or water clarity (Olmanson *et al.* 2008), turbidity (Petus *et al.* 2009) and water temperature (Giardino *et al.* 2001), among others. The empirical approach is distinguished from bio–optical model–based approaches by directly relating the remote sensed signal to the parameter of interest using statistical techniques. The great number of recent studies using this approach proves that empirical algorithms have the capacity to provide reliable information on inland and transitional waters. Table 1 provides a comprehensive (but not exhaustive) overview of recent studies using empirical methods for quantitatively estimating a variety of biogeophysical parameters from spaceborne, airborne and *in situ* remote sensing instruments in inland and transitional waters. Table 1 gives information from each study on: the location, the remotely sensed data type(s), the atmospheric correction procedure(s) (if applicable), the estimated water quality parameter(s), the range of the parameter(s), the statistical technique(s) used to derive the algorithm(s), the band(s)/band ratios/arithmetic independent variable(s), the coefficient of determination ($r^2$), the root mean square error (RMSE), and the sample size (N). In some instances only one best performing or key algorithm from a study is included. The table is arranged by instrument in the following order: studies using dedicated 'ocean colour' sensors, e.g. MODIS, MERIS or simulations of these; studies using high resolution sensors, e.g. Landsat, or simulations of these; and studies using hyper/multispectral satellite and airborne platforms and *in situ* radiometers. The aim of the review is to describe the current status of empirical remote sensing in inland and transitional waters, and identify remotely sensed band(s), band ratios and band arithmetic variables suitable for detecting specific parameters using certain instruments and statistical approaches in different water types. These are identified for their potential to provide common information products on inland and transitional waters using an empirically-based approach. Special emphasis is given to explaining the basis of these algorithms in terms of the inherent optical properties (IOPs), the absorption and backscattering coefficients of the optically-active water constituents, phytoplankton, CDOM, detritus and minerals. In doing so a theoretical basis for the algorithms is established using simple bio-optical theory: this is crucial for the cross-applicability and generalizability of the algorithms. The paper begins with an overview of remote sensing instruments as applicable to inland and transitional waters. It then gives a detailed review of empirical algorithms arranged according to the various biogeophysical parameters for various instruments and an explanation of their success in terms of simple bio-optical theory. The review ends by recommending empirical algorithms for common use and by discussing the role such algorithms could play alongside more advanced model-based approaches in the future of water remote sensing. This paper should provide a useful reference of empirical algorithms for workers for a variety of ecosystem and monitoring applications.

**Table 1 – see Appendix**

## 2. Remote sensing instruments and their application to inland and near coastal transitional waters.

Passive remote sensing instruments, whether hand-held or mounted on aircraft or satellites, measuring the light in the visible and near-infrared (NIR) part of the electromagnetic spectrum (400 to 1000 nm) are most often used for water-related applications. The optically-active water constituents including phytoplankton, *tripton* made up of detritus and minerals, CDOM (also called *gelbstoff* or yellow substances) and water itself all have an impact on the optical signature of water in the visible wavelengths. Viruses, bacteria, bubbles and other aqueous particles may also be significant (see Stramski *et al.* 2004) but are generally not routinely detected. The water-leaving radiance is modified through the backscattering ($b_b$) and absorption ($a$) of light by these constituents (called the IOPs) (Preisendorfer 1976). Absorption by phytoplankton, $a_\Phi$, *gelbstoff* and detritus, $a_{dg}$, and water, $a_w$, are well defined (Figure 1) and can be used to explain the causal relationships between the observed remote-sensing reflectance and the biogeophysical parameter(s) of interest in terms of bio-optical theory (see Kirk 1994). The backscattering coefficients for water, $b_{bw}$, minerals, $b_{bm}$, phytoplankton, $b_{b\phi}$, and particulate matter, $b_{bp}$, (negligible for *gelbstoff* and detritus) may be used in the same way. Strong absorption by water at wavelengths >~750 nm (Buiteveld *et al.* 1994) effectively masks out the signals from other constituents except in highly turbid water where scattering by minerals overwhelms absorption by water. Therefore wavelengths between 400 and 750 nm generally contain the most information on the water constituents which is detectable by remote sensing instruments, with the exception of highly turbid water where the signal in the NIR is also useful.

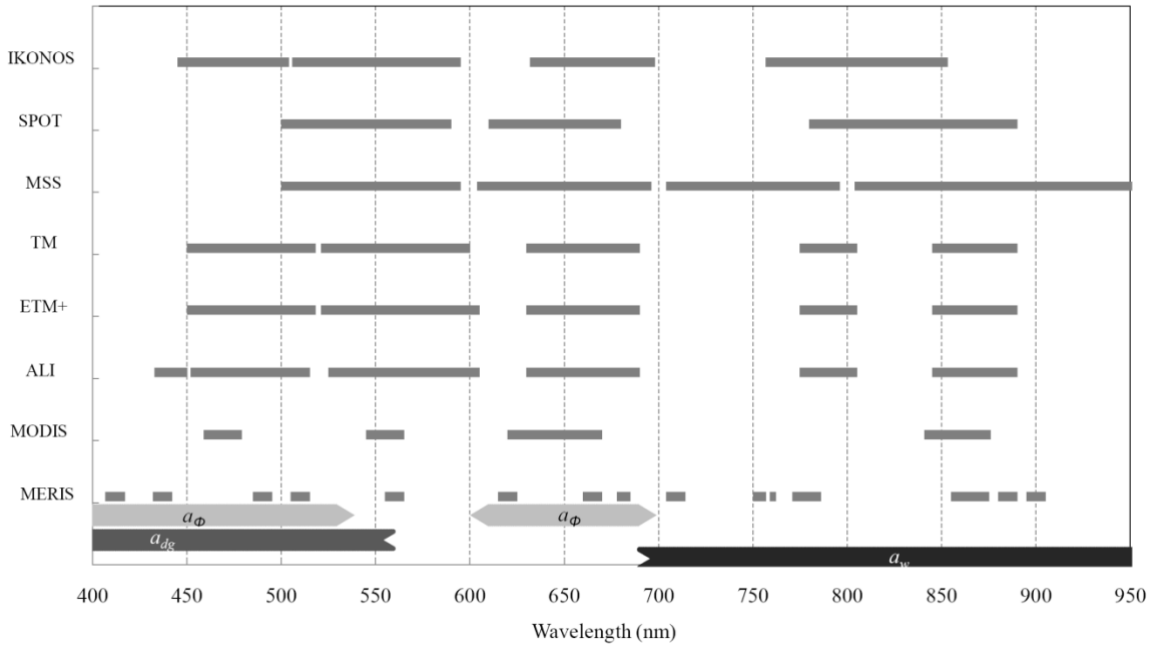


Figure 1. The spectral position of various satellite instruments in relation to the location of the maximum influence of absorption by phytoplankton, $a_\Phi$, detritus and *gelbstoff*, $a_{dg}$, and water, $a_w$. The bands plotted for MODIS are the 250 and 500 m bands.

Portable field spectroradiometers typically used for *in situ* calibration/validation purposes provide multi-/hyperspectral measurements (up to 1 nm resolution) of the upwelling radiance above the water, or just beneath the surface, and the downwelling irradiance above the surface. There are a wide range of spectroradiometers available: commonly used instruments include the PR-650 SpectraColorimeter (Photo Research, Chatsworth, CA) (Gons *et al.* 2002, Giardino *et al.* 2007, Simis *et al.* 2007); the TriOS-RAMSES radiometers (TriOS Optical Sensors, Germany) (Doxaran *et al.* 2005, Ruddick *et al.* 2006, Neukermans *et al.* 2009); and the ASD FieldSpec spectroradiometer (Analytical Spectral Devices, Inc. Boulder, CO, USA) (Ruiz-Verdú *et al.* 2005, Jiao *et al.* 2006, Simis *et al.* 2007). *In situ* hyperspectral reflectance/radiance measurements have been essential not only for calibration/validation of the water-leaving reflectance derived from satellite/airborne measurements, but also for the derivation of empirical algorithms (e.g. Gitelson *et al.* 1993, Doxaran *et al.* 2002, Zimba and Gitelson 2006). The findings of these and similar studies form the basis for algorithm development and are therefore a vital component in the development of remote sensing systems.

Space and airborne remote sensing instruments used for inland and near coastal water-related applications must meet the minimum spectral, spatial, temporal, radiometric and signal-to-noise ratio (SNR) requirements. The detection of certain water constituents, such as phytoplankton pigments, e.g. Chl *a*, necessitates that the remote-sensing reflectance be resolved in sufficient detail for the application of suitable detection algorithms. The ground resolution of a pixel for larger inland waters (>~1 $km^2$) should be a few hundred meters or less, several times larger than the dimensions of the target. Also the sampling frequency should be regular, especially when considering that cloud cover may substantially reduce the number of useful images. Higher radiometric resolutions and SNRs are also required to sufficiently describe the low range of reflectance values over water. In large, these sensor requirements are dictated by the intended application: ecosystem analysis applications generally require higher sampling frequencies to resolve system changes occurring over short time-scales (days/weeks), and high SNRs to improve confidence limits; course change detection applications with larger signals, such eutrophic status determination, are generally accommodated with more coarse radiometric resolutions and lower overpass frequencies. Therefore the selection of the remote sensing instrument is based on the desired application, e.g. operational phycocyanin detection from currently available high-spatial resolution satellite sensors may not be feasible (see 4.5.3).

Table 2.
Current earth observation satellite sensors which may be used for water quality assessments in inland and near-coastal waters showing resolution specifications and full names. Italics indicate scheduled sensors.

| Satellite | Sensor | Spectral resolution (μm) | Spatial resolution | Temporal resolution | Example of study |
|---|---|---|---|---|---|
| LM900 | IKONOS | 0.45-0.85 (4 bands) | 4 m | 3/5 days | (Hellweger *et al.* 2007) |
| IRS-P6 | LISS 4 | 0.52-0.68 (3 bands) | 5.8 m | 5 days | - |
| SPOT 5 | HRG | 0.48-1.75 (5 bands) | 10 m | 26 days | (Dekker *et al.* 2002) |
| Proba-1 | CHRIS | 0.415-1.050 (19 bands) | 18 m | ~ 7 days | (Miksa *et al.* 2004) |
| SPOT 4 | HRVIR | 0.50-0.89 (3 bands) | 20 m | 26 days | (Lathrop and Lillesand 1989) |
| IRS-P6 | LISS 3 | 0.52-1.70 (4 bands) | 23.5 m | 24 days | (Thiemann and Kaufmann 2000) |
| *EnMAP* | *HSI* | *0.420 – 2.450 (200 bands)* | *30 m* | *4 days* | - |
| EO-1 | Hyperion | 0.4-2.5 (220 bands) | 30 m | 16 days | (Giardino *et al.* 2007) |
| EO-1 | ALI | 0.43-2.35 (9 bands) | 30 m | 16 days | (Kutser *et al.* 2005) |
| Landsat 5 | TM | 0.45-2.35 (6 bands) | 30 m | 16 days | (Vincent *et al.* 2004) |
| Landsat 7 | ETM+ | 0.45-2.35 (8 bands) | 30 m | 16 days | (Olmanson *et al.* 2008) |
| ISS | HICO | 0.3 - 1.0 (128) | 100 m | - | |
| Terra/Aqua | MODIS | 0.620-0.876 (2 bands) | 250 m | 1-2 days | (Chen *et al.* 2007) |
| EnviSAT | MERIS | 0.412-0.900 (15 bands) | ~300 m | 2-3 days | (Giardino *et al.* 2005) |
| *Sentinal 3* | *OLC* | *0.413-1.020 (16 bands)* | *~300 m* | *2-3 days* | - |
| IRS-P4 | OCM | 0.400-0.885 (8 bands) | 360 m | 2 days | - |
| *COMS* | *GOCI* | *0.400-0.900 (8 bands)* | *500 m* | *~ 15 mins* | - |
| *TRAQ* | *OCAPI* | *0.320 - 2.13 (8 bands)* | *4km* | *14 mins* | - |
| SeaWiFS | WiFS | 0.402-0.885 (8 bands) | 1 km | 2 days | (Vos *et al.* 2003) |

| Abbreviation | Full name |
|---|---|
| ALI | Advanced Land Imager |
| CHRIS | Compact High Resolution Imaging Spectrometer |
| COMS | Communication, Ocean, and Meteorological Satellite |
| ETM | Enhanced Thematic Mapper |
| GOCI | Geostationary Ocean Colour Imager |
| ISS | International Space Station |
| HICO | Hyperspectral Imager for the Coastal Ocean |
| HRVIR | High Resolution Visible and Infra Red imaging instrument |
| HRG | High Resolution Geometric imaging instrument |
| IKONOS | Derived from the Greek word for 'image' |
| LISS | Linear Imaging Self-Scanning Sensor |
| MODIS | Moderate Resolution Imaging Spectrometer |
| MERIS | Medium Resolution Imaging Spectrometer |
| OCAPI | Optical Carbonaceous and anthropogenic Aerosols Pathfinder Instrument |
| OCM | Ocean Colour Monitor |
| OLC | Ocean and Land Colour Imager |
| SeaWiFS | Sea-viewing Wide Field-of-view Sensor |
| TM | Thematic Mapper |
| TRAQ | TRopospheric composition and Air Quality |

Airborne platforms typically carry multi-/hyperspectral spectrometers capable of capturing many spectral bands. Hyperspectral instruments can be used to derive an almost continuous spectrum of the surface reflectance. Examples of airborne sensors commonly used in inland waters are the Airborne Imaging Spectrometer for Applications (AISA) (Härmä *et al.* 2001, Kallio *et al.* 2003) and the Compact Airborne Spectrographic Imager (CASI) (Ammenberg *et al.* 2002, Hunter *et al.* 2009). The data from these sensors are particularly useful since the spectral widths and positions can normally be adjusted to suit the intended application, or re-sampled to simulate multispectral satellite sensors that have broader and fewer bands. The very high spectral resolution presents opportunities for applications that are not feasible with sensors with few

and broad bands, such as the determination of algal species composition through the detection of specific algal pigments, for example phycocyanin pigment present in cyanobacteria (Richardson 1996, Gege 1998, Hunter *et al.* 2008). The spatial resolution of most airborne sensors is also high, given the low altitude that the images are acquired, and the contribution from the atmosphere is often presumed to be negligible which means that atmospheric correction may sometimes be ignored. However, atmospheric correction is nevertheless required when using algorithms based on $R_{rs}$. Furthermore, airborne campaigns can be timed to coincide with events such as blooms, tides, floods and other episodic events providing more flexibility than satellite sensors. There are numerous recent examples where airborne sensors have been used successfully for the detection of various water quality parameters in lakes (e.g. Dierberg and Carriker 1994, Hakvoort *et al.* 2002, Koponen *et al.* 2002, Floricioiu *et al.* 2003, Hunter *et al.* 2009, Table 1). However, the difficulty in obtaining temporally and spatially consistent data as acquired from satellites, and the relatively high cost of campaigns, makes this approach generally unsuited to frequent monitoring applications, especially in the developing world.

Satellite platforms offer substantial advantages over airborne platforms mainly because of the temporal and spatial consistency, larger area coverage and reduced data cost borne over a large user community (Rees 2001). There are a number of current and scheduled earth-observation satellites that may be used for water quality monitoring (see Table 2). Hyperspectral satellite-based sensors are only now progressing beyond the experimental phase owing to constraints related to instrument design (SNR), difficulties with atmospheric correction, and the large quantities of data that must be transmitted and stored. The first experimental hyperspectral sensor to orbit the earth in space was the Hyperion imaging spectrometer, launched in 2001, and has been used for deriving detailed water quality parameters in inland and near-coastal transitional waters (Brando and Dekker 2003, Kutser 2004, Giardino *et al.* 2007). Hyperion has 220 bands between 0.4 and 2.5 μm, a spatial resolution of 30 m, and an overpass time equivalent to the Landsat sensors (16 days). Hyperion is now near the end of its life span and does not acquire images routinely. The recently launched experimental Hyperspectral Imager for the Coastal Ocean (HICO) on board the International Space Station is designed specifically for monitoring the littoral coastal environment and has been acquiring imagery since September 25$^{th}$ 2009. HICO has a high SNR and a ground resolution of 90 m, making it suitable for lakes (Corson *et al.* 2008). Similar sensors are likely to be used increasingly in the future (for example, the Enmap Hyperspectral Imager scheduled for launch in 2012). High/medium resolution spectrometers with fewer bands than hyperspectral sensors, such as the experimental Compact High Resolution Imaging Spectrometer (CHRIS) on board the Proba-1 platform, have also been used for water quality monitoring (Miksa *et al.* 2004, Ruiz-Verdú *et al.* 2005). CHRIS has 19 bands in 'water mode' ideally positioned for water-related applications, a spatial resolution of 18 m (swath width is only about 14 km) and an image acquisition frequency of about seven days. However, as CHRIS is only an experimental sensor, actual data acquisition may be infrequent due to conflicting demands of different sites for images, and there are also substantial challenges related to atmospheric correction. It is likely that other spectrometers with high spectral definition and spatial resolution, and fairly regular image acquisition, will be used increasingly in future.

Multi-spectral sensors such as IKONOS, LISS 3 and 4, SPOT 4 and 5, Landsat 5 and 7, and ALI, have few, broad bands and high spatial resolutions (4–30 m) and are primarily designed for terrestrial applications (see Table 2, Figure 1). Nonetheless, there are a great number of successful studies which use these instruments to estimate a variety of water quality parameters in inland/transitional waters (e.g. Thiemann and Kaufmann 2000, Dekker *et al.* 2001, Chang *et al.* 2004, Vincent *et al.* 2004, Wang *et al.* 2004, Kutser *et al.* 2005a, Doxaran *et al.* 2006, Hellweger *et al.* 2007 table 1). These instruments offer the advantage of being able to view even very small lakes with high spatial definition. However, the spectral and radiometric configuration (broad bands, low SNR) of these instruments generally limits their usefulness to course change detection studies: the broad spectral bands impede the detection of certain parameters, and the absence of NIR bands (in some sensors) make atmospheric correction more challenging. The low acquisition frequencies (with the exception of constellations, e.g. SPOT) mean that they are better suited to event-scale, rather than frequent change detection applications. In general, these instruments are used for deriving site-and-time parameter specific empirical algorithms – although the cross-applicability of algorithms for certain parameters has been shown (e.g. Dekker *et al.* 2002, Doxaran *et al.* 2006, Olmanson *et al.* 2008). For operational purposes, data cost from these instruments is a significant concern – although there are exceptions such as Landsat which is available free of charge including for countries in the developing world, although some of the data is unusable due to the SLC failure and the archive is sporadic (NASA 2008).

Typical 'ocean-colour' sensors more suited to real-time operational and detailed parameter retrieval, such as MODIS, SeaWiFS, OCM and MERIS, have high acquisition frequencies, bands ideally positioned for the detection of water constituents and atmospheric correction, and high SNRs (see Table 2, Figure 1). The obvious disadvantage of these sensors for inland waters is their lower spatial resolution, typically between 250 and 1000 m in full resolution mode. The spatial resolution of SeaWiFS and MODIS ocean colour bands (1 km) is too low for all but the largest inland lakes (Vos *et al.* 2003, Chavula *et al.* 2009). MODIS's two broad high resolution bands (250 m) have been used successfully for monitoring TSS and for water classification in inland lakes and estuaries (Koponen *et al.* 2004, Miller and McKee 2004, Chen *et al.* 2007, Doxaran *et al.* 2009, Petus *et al.* 2009). However, its ability to detect other crucial parameters, such as phytoplankton pigments (Chl *a*) is limited. MERIS is perhaps the best suited of these sensors for inland water quality monitoring with a full resolution of ~260 by 290 m and 15 bands in the visible and NIR. There are several examples using MERIS in inland and near-coastal waters (e.g. Floricioiu *et al.* 2004, Giardino *et al.* 2005, Koponen *et al.* 2007, Kratzer *et al.* 2008, Odermatt *et al.* 2008, Moses *et al.* 2009a). The availability of a standard MERIS Level 2 product suited for use in coastal waters (Schiller and Doerffer 1999, Schiller and Doerffer 2005) and products for regional case 2 waters and lakes (Doerffer and Schiller 2008a, Doerffer and Schiller 2008b) is very convenient for a variety of studies – although these algorithms require parameterisation to work in different regions. Recent research shows that MERIS may even be used in small lakes with equal or more effectiveness than Landsat which makes it arguably the current optimal sensor for inland water monitoring (Matthews 2010). Data from these ocean colour sensors are also available free for research purposes, making them a more viable option for scientists, particularly in the developing world.

The proposal of using geostationary satellite sensors to monitor parameters such as TSS has already been proved using the SEVERI sensor onboard METEOSAT Second Generation (Neukermans *et al.* 2009, Salama and Shen 2010). Future dedicated ocean colour geostationary sensors such as the Global Ocean Colour Imager (GOCI) (Korean Aerospace Research Institute) (Kang *et al.* 2006) the Optical Carbonaceous and anthropogenic Aerosols Pathfinder Instrument (OCAPI) (CNES/ESA) (Le Naour *et al.* 2006) and the Geostationary Coastal and Air Pollution Events sensors (GEO-CAPE) (NASA) (Al-Saadi *et al.* 2009) will be capable of providing almost continuous data (~ 15 mins) – the main challenges are related to radiometric resolution and sensitivity due to the distance from the target (Kang *et al.* 2006).

## 3. Quantitative remote sensing of biogeophysical water quality parameters.

Broadly, there are two approaches for deriving water quality products from remotely sensed data: the empirical and model-based approaches. The model-based (or analytical) approach seeks to model the remote-sensing reflectance, $R_{rs}(0+)$, (or the reflectance at the top of the atmosphere, $R_{TOA}$) in terms of the water IOPs through radiative transfer modelling (see Dekker *et al.* 2001 for an overview) (See Figure 2).

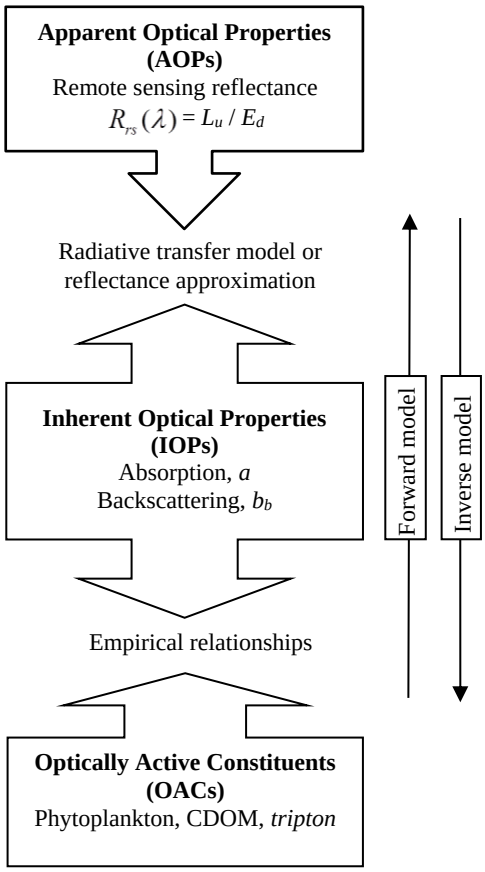


Figure 2. Simplified schematic diagram of the forward and inverse models used in model-based approaches.

The 'forward' model derives $R_{rs}(0+)$ from the water IOPs using a bio-optical model and an approximation of the radiative transfer equation, called the reflectance approximation (Morel and Prieur 1977, Zaneveld 1995), or through direct solution of the RTE using models such as Hydrolight (Mobley 1994). The $R_{TOA}$ can then be modelled using radiative transfer calculations for the atmosphere through codes such as 6S (Vermote *et al.* 1997) or MODTRAN (Kneizys *et al.* 1988). The 'inverse' model solves for the IOPs (or concentrations of optically-active water constituents) from reflectance measured at the TOA by satellites or from *in situ* measurements of $R_{rs}(0+)$. The 'inversion' problem may be solved using any of a variety of mathematical optimisation or multiple non-linear regression procedures, such as Artificial Neural Networks, to produce 'analytical' or 'inversion' algorithms (IOCCG 2000, IOCCG 2006). This allows for a number of parameters to be solved for simultaneously, most often $a_\Phi$ (which may be converted to the concentration of Chl *a*), backscattering from suspended solids, $b_{bp}$, and $a_{CDOM}$, independent of simultaneously acquired experimental data (e.g. Odermatt *et al.* 2008). The European Space Agency's MERIS Lakes and Case 2 Processors, such as the Eutrophic Lakes Processor, are examples of operational inversion type algorithms for use in inland waters (Doerffer and Schiller 2008a, 2008b) The main concerns with these kinds of algorithms are their sensitivity to errors from atmospheric correction procedures (e.g. Lee *et al.* 2002), and the existence of non-unique or ambiguous solutions arising from the additive nature of the IOPs and the consequences of using a ratio in the reflectance approximation (Defoin-Platel and Chami 2007). The analytical approach is generally complex and ideally requires measurements and knowledge of local/regional IOPs to develop a robust forward model. This often requires substantial fieldwork and algorithm training and computing time. As this review focuses on the empirical approach, analytical algorithms are beyond the scope of this paper and reviews can be found elsewhere (see IOCCG 2000, IOCCG 2006). Closely related to the analytical approach is what is often called the semi-analytical approach which uses algebraic solutions of the reflectance approximation to derive biogeophysical parameters (e.g. Gons *et al.* 1999, 2002, Simis *et al.* 2005, and others). Some studies using the semi-analytical approach are included in this review because they have rather simple algebraic solutions and

are also useful for understanding the causal relationship between the remote sensing reflectance, the IOPs, and the parameter of interest.

In contrast to the analytical approach, empirical algorithms are relatively simple to derive and use: simultaneously acquired experimental sets of limnological, atmospheric, and remotely sensed data are used to derive normally site-and-time specific algorithms for a certain parameter using statistical regression techniques. These algorithms generally produce robust results for the areas and data sets from which they are derived. Figure 3 shows a simplified schematic diagram of the main steps used in the empirical approach.

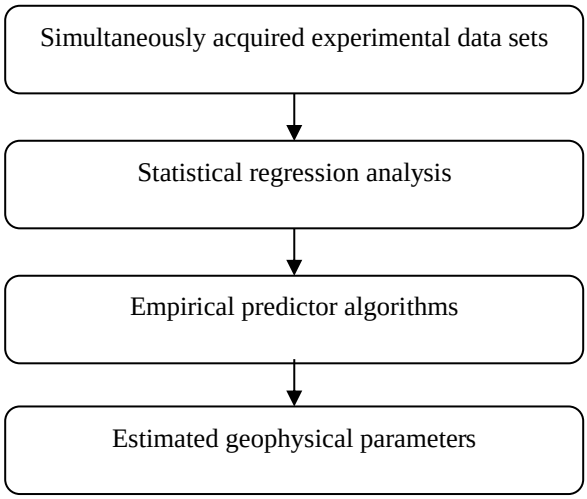


Figure 3. A simplified schematic diagram of the empirical approach for deriving geophysical water quality parameters from remotely sensed data.

The first step involves the collection of simultaneous sets of remotely sensed, atmospheric and biogeophysical water quality parameter data (this may also include IOPs, e.g. the total absorption coefficient, $a$, or backscattering from particulate matter, $b_{bp}$). The acquisition of all these data simultaneously requires substantial effort especially when considering that cloud cover may significantly reduce the number of successful match-ups. After collection the data must be processed to a form suitable for the intended application. This may include atmospherically correcting the TOA radiances to surface reflectances, which may be performed using a variety of techniques (see Table 1). The next step is to determine correlations between the remotely sensed data and the water quality parameter of interest which may be achieved using linear, multiple-linear, nonlinear or other statistical models. This leads to the derivation of an empirical algorithm which may be used to estimate the spatial distribution of the parameter from the remotely sensed data. A good example of a commonly used empirical algorithm is the colour-ratio algorithm which uses a ratio of the reflectance, $R_i$, in two spectral channels, $i$, to estimate the parameter, $p$, where $\alpha$, $\beta$, and $\gamma$ are regression coefficients (IOCCG 2000):

$$p = \alpha \frac{R_1}{R_2}^{\beta} + \gamma \qquad (1)$$

There are many varieties of algorithms that use either single bands, band ratios, band arithmetic or multiple bands as independent variables in linear, multiple linear or nonlinear regression analyses (Table 1). Once the algorithm has been parameterised it may be applied to remotely sensed data to estimate the spatial distribution of the parameter in the form of a map. This step usually assumes that the water and atmospheric conditions remain constant throughout the scene. Should the algorithm be applied to scenes acquired at different times or over different areas the relative errors in the parameter estimates will generally increase as these assumptions break down. The empirical approach when compared to the inverse modelling approach has the key advantages

of computational simplicity and ease of implementation. For these reasons it makes up the majority of studies in inland waters. Normally, empirical algorithms can be expected to perform well only inside their range of derivation and for the area for which they are derived. They are also more limited in their ability to discriminate between non-unique signals from parameters that may be covariant, e.g. TSS and Chl *a*, than inversion algorithms which solve for a number of parameters simultaneously. Empirical algorithms for estimating $z_{SD}$, TSS, Chl *a*, $a_{CDOM}$, and other parameters from recent studies in inland and near-coastal transitional waters are reviewed below. The parameters are arranged to reflect the increasing complexity in the methods used. An explanation of the choice of independent variables (bands/band ratios) is often lacking or missing in many empirical studies. This paper has attempted to fill this gap by providing brief explanations for the basis of the algorithms in terms of the effect of the IOPs on the remote sensing reflectance. For other reviews of empirical algorithms see Kirk (1994), Durand *et al.* (1999), Lindell *et al.* (1999) and (Kutser 2009).

## 4. Review of empirical algorithms.

### *4.1 Secchi disk algorithms.*

Secchi Disk depth ($z_{SD}$) is defined as the depth, in metres, at which a circular white disk disappears when lowered into water as perceived by the human eye, and is a measure of the depth of penetration of light in the water or water clarity (Preisendorfer 1986). $z_{SD}$ is inversely proportional to the average amount of inorganic and organic material in the water. Therefore, $z_{SD}$ is a proxy for gross particulate load, or in humic lakes the concentration of dissolved organic matter, which is known to have a large effect on water-leaving radiance. $z_{SD}$ derived from remotely sensed data essentially shows changes in gross particulate load, which is useful for obtaining information on biological activity (trophic status) and sediment flux. Thus Secchi disk is a valuable quantity for aquatic scientists and is also important from a water management perspective as water clarity is often the basis with which water users perceive water quality.

There are a large number of studies using Landsat to retrieve $z_{SD}$ and most of these use simple linear regressions of single bands or band ratios. In particular, the use of the red TM3 band is ubiquitous (as single band or ratio) (e.g. Lathrop 1992, Pattiaratchi *et al.* 1994, Cox *et al.* 1998, Härmä *et al.* 2001, Hellweger *et al.* 2004, Kallio *et al.* 2008, Wu *et al.* 2008, Duan *et al.* 2009). In almost all cases the relationship of $z_{SD}$ to brightness is non-linear – and therefore $z_{SD}$ is log transformed in regressions. The correlation with the red band may be causally explained by the direct positive correlation between reflectance in the red and gross particulate load inducing particulate scattering. Therefore, as water clarity ($z_{SD}$) decreases brightness in the red usually increases. Among these studies, a ratio using the reflectance in the red, TM3, to that in the blue, TM1, is particularly common. 'Ratioing' using the blue band, which is dominated by the absorbing effects of phytoplankton, *gelbstoff* and detritus, serves to normalise the brightness in the red band (see Figure 1). TM1 is least correlated with $z_{SD}$ because of the offset to scattering by strong absorption in the blue. A possible exception may be for very clear lakes (e.g. Giardino *et al.* 2001 who used TM1) or for humic lakes – although the very small signal in the blue in these conditions may render it unusable (e.g. Härmä *et al.* 2001). Building on the TM3/TM1 ratio, many studies have subsequently included an additional variable in the form of TM1 (or TM3) in a multiple linear regression to achieve higher correlations (Lavery *et al.* 1993, Kloiber *et al.* 2002, Brezonik *et al.* 2005, Olmanson *et al.* 2008). Thus a multiple regression of the form TM3/TM1 + TM1 may become a common equation for assessing $z_{SD}$ using Landsat owing to the consistency of the algorithms performance (Kloiber *et al.* 2002). There are some examples which use green (Lathrop and Lillesand 1986) or NIR bands (SPOT) (Lathrop and Lillesand 1989), although there are few recent examples of this. Less causally explicable multiple regressions with many bands have also been used (Alparslan *et al.* 2007), as well as more advanced approaches such as Principal Component Analysis (Wang and Ma 2001) and artificial neural networks (Zhang *et al.* 2002).

Typical narrow band ocean colour sensors such as MODIS and MERIS have also been used successfully to estimate $z_{SD}$ in lakes and near-coastal transitional waters, with red bands again being used most often. For lakes and coastal waters in Finland, a ratio of the MERIS blue band at 521 or 492 nm to the red band at 620 or 700 nm proved to give the highest correlations (up to 0.93) (Härmä *et al.* 2001, Kallio *et al.* 2001, Koponen *et al.* 2002, Kratzer *et al.* 2008). The subtraction of a NIR band from each of the bands in some of these studies acts as a rough correction for atmospheric effects. These results again confirm the agreeableness

of the blue to red ratio for estimating $z_{SD}$. It appears that the lack of studies utilising MODIS to derive water clarity in inland/transitional waters is a results of the relatively course resolution of some of the broad visible bands (e.g. bands 3 and 4 are 500 m). However, given the high coefficients of determination observed with the 250 m red band 1 (e.g. Wu *et al.* 2008), and the frequency of acquisition and large quantity of archived data, MODIS has much latent potential to give information on the historical and future trends of water clarity in the world's inland and coastal waters.

### *4.2 Total suspended solids algorithms*

Total Suspended Solids (TSS) (also called total suspended matter or suspended matter) is the name given to the total mass of suspended particles as measured per volume of water including inorganic (minerals) and organic (detritus and phytoplankton) components. TSS is important for water quality management since it is related generally to primary production, sediment transport and more specifically to water clarity/opacity which is an indicator of water quality (Dekker *et al.* 2002). It is apparent however that far fewer studies investigate TSS compared to Chl *a*, and finding empirical algorithms that effectively separate the signals from TSS and Chl *a* can be challenging.

A difference ratio algorithm of the form ($R560–R520$)/($R560+R520$) was found to be highly correlated with TSS in lakes and rivers not exceeding 66 $g.m^{-3}$ (Gitelson *et al.* 1993). The algorithm takes advantage of the phytoplankton absorption minimum near 560 nm which makes the reflectance there sensitive to changes in TSS, while the reflectance at 520 nm is relatively insensitive to changes in TSS (Figure 1). Thus the difference ratio acts to normalise the signal at 560 nm for scattering by TSS. More recently, Doxaran *et al.* (2002) have shown that by exploiting the increased scattering from TSS in the NIR in the highly turbid (<985 $g.m^{-3}$) waters of the Gironde Estuary, France, a ratio of the reflectance near 850 nm to that at about 550 nm also exhibits a strong non-linear correlation. This result shows the high potential of NIR bands for TSS estimations, as will be shown later on in the discussion. TSS has also been estimated using the reflectance peak near 700 nm much like Chl *a* from sensors such as MERIS in relatively low concentrations less than 32 $g.m^{-3}$ ($r^2$>0.81) (Härmä *et al.* 2001, Kallio *et al.* 2001, Koponen *et al.* 2007). However, this may give rise to significant ambiguity between TSS and Chl *estimations* from satellite data especially when they are, as they often are, significantly covariant.

The retrieval of TSS from broad-band sensors (including the broad MODIS 250 m bands 1 and 2) has in general been more successful than that of Chl *a* in terms of significance of correlations (Lathrop and Lillesand 1989, Dekker *et al.* 2002, Doxaran *et al.* 2002, Doxaran *et al.* 2006, Onderka and Pekarova 2008, Doxaran *et al.* 2009, Petus *et al.* 2009). In many instances simple linear regressions of single bands and band ratios give sufficiently good correlations ($r^2$>0.82) (Östlund *et al.* 2001, Doxaran *et al.* 2002, Miller and McKee 2004, Sváb *et al.* 2005, Doxaran *et al.* 2006, Tyler *et al.* 2006, Onderka and Pekarova 2008, Doxaran *et al.* 2009). However, there is no immediately apparent agreement between studies reviewed here on which bands/ratios are best for TSS estimation. Lathrop and Lillesand (1989) found that at high concentrations (>10 $g.m^{-3}$) the red (XS2) and NIR (XS3) bands of SPOT 1 HRV are more sensitive to changes in TSS than at low concentrations, where a ratio of red to green (XS2/XS1) proved more sensitive. Thus they uses a multispectral approach by combining the red to green ratio and the NIR band to account for the entire data range (4.6–28.9 $g.m^{-3}$, $r^2$ = 0.93). The usefulness of single red and NIR bands has been confirmed over similar concentrations by other studies including those using the MODIS 250 m bands 1 (620–670 nm) and 2 (841–876 nm) (e.g. Miller and McKee 2004, Tyler *et al.* 2006, Onderka and Pekarova 2008, Petus *et al.* 2009). More recent work by Nechad *et al.* (2010) used bio-optical theory to prove the usefulness of single red or NIR band algorithms for estimating TSS in turbid waters from MERIS, MODIS and SeaWiFS. The proof of concept of using the single visible band (600–700 nm) of the geostationary SEVERI onboard METEOSAT Second Generation to estimate TSS has already been confirmed (Neukermans *et al.* 2009, Salama and Shen 2010). The reason for the correlation is explained by the contribution of particulate matter, particularly the inorganic component, to scattering in the red and NIR.

However, Dekker *et al.* (2002) pointed out that for Landsat, the sensitivity is lower, radiometric calibration less reliable, and the influence of the adjacency effect more severe in the NIR, citing potential drawbacks of using a single Landsat TM NIR band (See also Ruddick *et al.* 2006). Nonetheless, it these

problems can be solved through new more advanced sensors and better atmospheric correction procedures, then single band NIR algorithms would be very effective for estimating TSS. Using a bio-optical modelling approach, Dekker *et al.* (2002) found that an exponential relationship between the average of the green and red bands of Landsat TM (TM2, TM3) and SPOT 3 HRV (XS1, XS2) was highly correlated ($r^2 = 0.99$) with TSS in the range 5–50 $g.m^{-3}$ for turbid lakes in the Netherlands. This algorithm takes advantage of the reflectance maximum near 560 nm in the green (explanation given above) and the increasing reflectance in the red, and avoids the current problems with using single NIR bands. In estuarine waters with very high concentrations of TSS (>2000 $g.m^{-3}$) Doxaran *et al.* (2002, 2003, 2006) showed through using a bio-optical model the robustness of the NIR to green and NIR to red band ratios for estimating TSS from SPOT over long time-scales. The use of band ratios, as opposed to the single NIR band, normalises (reduces) the effects of variable sediment refractive indices and particle grain-sizes. Thus there may be advantages using ratios over single bands in instances where algorithms are expected to perform well over large variations in TSS caused by tidal or seasonal variations, such as occurs in estuaries (e.g. Doxaran *et al.* 2009). From the above examples, it would appear that the choice of algorithm for TSS when using broad-band sensors largely depends on the concentration ranges and area of investigation.

An alternative approach to estimating TSS is to use multiple linear regressions (e.g. Wang and Ma 2001, Wang *et al.* 2006, Alparslan *et al.* 2007). Although these procedures may give high coefficients of determination, they lack usually causal explanations and cross-temporal applicability of those reviewed already. More advanced type algorithms such as artificial neural networks (discussed further below) using multiple bands have also been used to improve retrieval accuracies (Zhang *et al.* 2002, Sudheer *et al.* 2006).

### *4.3 Phytoplankton pigment algorithms (Chl a).*

Phytoplankton pigment concentration (Chl *a*) is the most commonly derived parameter in water quality remote sensing mainly because of its use in determining the trophic status of waters. It acts as a proxy for phytoplankton concentration and is therefore an important component in the derivation of secondary products such as primary production.

**4.3.1 R700/R670 based colour ratio algorithms.** The ratio of reflectance at about 700 nm to that near 670 nm has been widely used for estimating Chl *a* concentration in high-biomass waters (see Table 1). In particular, studies by Mittenzwey *et al.* (1992), Gitelson *et al.* (1993), and Gons *et al.* (1999) and more recently Moses *et al.* (2009) show that the correlation between Chl *a* concentration and the ratio is very significant ($r^2 > 0.8$) for a variety of waters including rivers, lakes, estuaries and in the laboratory, and over a wide range of concentrations from about 0.1–350 $mg.m^{-3}$. There are a large number of studies which use high spectral resolution airborne and *in situ* radiometric data (Dierberg and Carriker 1994, Jiao *et al.* 2006, Duan *et al.* 2007, Hunter *et al.* 2008, Hunter *et al.* 2009) to estimate Chl *a* using the ratio, and the $r^2$ values for these studies range from 0.75 (Duan *et al.* 2007) to 0.99 (Menken *et al.* 2006). The positioning of the MERIS' bands at 665 nm and 709 nm makes MERIS ideally suited for predicting Chl *a* using this ratio and many studies have recently been carried out (Flink *et al.* 2001, Härmä *et al.* 2001, Kallio *et al.* 2001, Ammenberg *et al.* 2002, Gons *et al.* 2002, Koponen *et al.* 2002, Kallio *et al.* 2003, Strömbeck *et al.* 2004, Gons *et al.* 2005, Koponen *et al.* 2007, Moses *et al.* 2009b) where coefficients of determination range from 0.84 (Flink *et al.* 2001) to 0.98 (Kallio *et al.* 2003). These studies generally use relatively simple linear, multiple-linear and non-linear power law regression or polynomial analyses.

The causal explanation for the strength of the correlation of Chl *a* with the 700/670 nm ratio is based on the interaction between backscattering from particulate matter (phytoplankton) and the strong absorption of water which both increase towards the infrared (Figure 1). The offset to scattering by absorption by water near 700 nm causes a sharp peak in highly scattering (turbid or productive) waters. The height and position of the peak is known to be well correlated with Chl *a*, with the peak shifting towards greater wavelengths (~715 nm) as Chl *a* increases (Gitelson 1992). In contrast, the reflectance near 670nm is uncorrelated with Chl *a* being almost constant owing to the Chl *a* absorption maximum which offsets backscattering. Thus the 700/670 nm ratio can be effectively exploited to determine Chl *a*, as it normalises the signal from particulate phytoplankton backscattering.

There are a number of studies which employ slight variations on the ratio. By subtracting a NIR band (781 or 754 nm) from the 709 nm and 665 nm bands as a rough atmospheric correction some of these studies improve the strength of the correlation (e.g. Härmä *et al.* 2001, Koponen *et al.* 2002). This is based on the assumption that the reflectance in the NIR over water is mainly due to atmospheric effects, which may be a false assumption over turbid water. Some studies make use of the height of the maximum reflectance peak near 700 nm ($R_{max}/R670$) rather than a fixed band width and have achieved high correlations ($r^2 = 0.95$) for a wide range of concentrations in Lake Kinneret, Israel (Yacobi *et al.* 1995). Others have used the peak near 560 nm rather than at 709 nm in low biomass conditions (Floricioiu *et al.* 2004, Candiani *et al.* 2005). Gons *et al.* (1999, 2002, 2005) restated the ratio in terms of the commonly used reflectance approximation (Morel and Prieur 1977) and used *in situ* reflectance and Chl *a* data to calibrate the value of the Chl *a* specific absorption coefficient, $a_{\phi}^{*}$, at 672 nm. This algorithm makes a number of assumptions including that the backscattering is spectrally invariant and can be sufficiently estimated from the NIR wavelengths. Nevertheless, the algorithm provides good results in well-mixed, high biomass waters. A more pronounced variation on the ratio is the so-called 'three-band model' proposed by Gitelson *et al.* (2003):

$$Chl\ a = R(\lambda_3)\left(\frac{1}{R(\lambda_1)} - \frac{1}{R(\lambda_2)}\right) \qquad (\text{mg.m}^{-3}) \qquad (2)$$

where $R(\lambda_1)$ is reflectance in wavelength maximally sensitive to Chl *a* absorption (670 nm), $R(\lambda_2)$ is reflectance in wavelength minimally sensitive to absorption by Chl *a* (710 nm), and $R(\lambda_3)$ is reflectance in wavelength minimally effected by absorption that accounts for scattering (750 nm).

The three-band algorithm has been used to give very good estimates of Chl *a* in turbid and very high biomass hypertrophic waters (Dall'Olmo and Gitelson 2005, Zimba and Gitelson 2006, Gitelson *et al.* 2008, Gitelson *et al.* 2009, Moses *et al.* 2009b). A new 'four-band' algorithm including an additional band near 700 nm was found to be an improvement over the three-band model in highly turbid lake water through better accounting for absorption by water and non-negligible scattering by suspended matter in the NIR (Le *et al.* 2009).

**4.3.2 The Fluorescence/Reflectance Line Height algorithm.** The fluorescence maximum near 685 nm has often been used to estimate Chl *a* (Gower 1980, Gitelson *et al.* 1994). The FLH algorithm measures the height of the fluorescence peak at 685nm from a linear baseline drawn between two points on either side of the peak (Dierberg and Carriker 1994, Giardino *et al.* 2005). The coefficients of determination for linear regression FLH algorithms range from 0.73 (Gitelson *et al.* 1994) to 0.86 (Dierberg and Carriker 1994) for Chl *a* concentrations not exceeding 79 $mg.m^{-3}$ in this instance. It is important to consider that the FLH algorithm is only suitable for use in relatively low-biomass waters (Chl a concentrations generally not exceeding about 30 $mg.m^{-3}$) as the backscattering peak near 700 nm overwhelms the fluorescence peak in high-biomass water. Therefore it is very difficult, or impossible, to differentiate between the signal from particulate backscattering and solar induced fluorescence in high biomass waters. A very similar algorithm that is better suited to high-biomass waters is the Reflectance Line Height (RLH) or Scattered Line Height (SLH) algorithm (Dierberg and Carriker 1994, Yacobi *et al.* 1995, Schalles *et al.* 1998). The RLH algorithm is a modified FLH algorithm and is written (after Gower *et al.* 1999):

$$RLH = L_2 - L_1 - \left((L_3 - L_1)\frac{(\lambda_2 - \lambda_1)}{(\lambda_3 - \lambda_1)}\right) \qquad (3)$$

where $L_i$ is the radiance in band $i$ and $\lambda_i$ is the centre wavelength of band $i$. Band $i = 2$ is centred on the reflectance peak close to 700 nm, while bands $i = 1, 3$ on either side determine the baseline (670 and 850 nm).

In waters with high Chl *a* concentrations, $r^2$ values range from 0.85 (Dierberg and Carriker 1994) to 0.96 (Yacobi *et al.* 1995). A minor variation on the RLH algorithm is the SUM algorithm, which uses the sum of the area under the reflectance peak using a baseline between 670 nm and 730 or 850 nm (Gitelson *et al.* 1994, Schalles *et al.* 1998). The SUM algorithm gave $r^2$ values greater than 0.84 for turbid productive waters (Schalles *et al.* 1998).

**4.3.3 Broad band algorithms.** Sensors such as Landsat, SPOT, and IKONOS, are often used to detect Chl *a* (e.g. Lathrop and Lillesand 1986, Dor and Ben-Yosef 1996, Thiemann and Kaufmann 2000, Giardino *et al.*

2001, Nas *et al.* 2009, Ormeci *et al.* 2009, table 1). However, the lack of narrow bands and low SNRs prevents the use of the more specialised algorithms already described. Therefore, simple linear regressions of single bands or band ratios (which may be log-transformed) are often used and occasionally give coefficients of determination as high as 0.98 (Lathrop and Lillesand 1986), but more often less significant correlations. There is little consistency between the studies concerning which band ratios or bands are useful to detect Chl *a*, with bands/ratios often selected in a seemingly haphazard manner. With a few exceptions (e.g. Gitelson *et al.* 1996, Brivio *et al.* 2001) there is often also no attempt to explain the observed correlation between bands/band ratios and Chl *a* causally. A ratio using the reflectance in the red band (TM band 3) and that in the blue (TM band 1) may be useful in this regard, as Chl *a* is directly proportional to the magnitude of the reflectance in band 3 due to the influence of the reflectance peak in the red, and inversely proportional to that in the blue, as a consequence of the chlorophyll absorption maximum in this wavelength (Gitelson *et al.* 1993, Gitelson *et al.* 1996, Han and Jordan 2005). Similarly a ratio using the red band and NIR band (TM band 4) gives some consistent results as the reflectance in the near-infra red may sometimes be assumed to be close to zero and less variable due to strong absorption by water (Yacobi *et al.* 1995, Duan *et al.* 2007). At lower Chl *a* concentrations (<20 $mg.m^{-3}$) it appears that the ratio of the green band (TM band 2) to the blue may be better suited as the correlation with Chl *a* shifts to slightly lower wavelengths in the red (Gitelson *et al.* 1993, Östlund *et al.* 2001). Another approach which gives good correlations in these conditions is to subtract the reflectance in the red from that in the blue to remove effects of scattering by inorganic suspended solids, and normalise using the green reflectance peak band (Mayo *et al.* 1995, Brivio *et al.* 2001). Normalising the reflectance in a band by integrating the reflectance in all visible bands (or the sum of the bands) may also lead to improved correlations (Gitelson *et al.* 1993). The alternative approach to these ratios is to use multiple linear regressions combining a number of bands or ratios, however a causal explanation is deficient and the cross applicability of these algorithms is normally very limited. Multiple variable linear regressions may use as many as four bands to give very high correlations (e.g. Giardino *et al.* 2001, Nas *et al.* 2009, Ormeci *et al.* 2009, table 1). More advanced and creative methods are then needed to establish causality and improve the cross-applicability of the procedures.

**4.3.4 Advanced algorithms.** Advanced algorithms are often employed in order to improve the strength of correlations and the cross-spatial/temporal applicability of algorithms. These include Artificial Neural Network algorithms (Zhang *et al.* 2002, Sudheer *et al.* 2006, Wu *et al.* 2009), genetic algorithms (Chen *et al.* 2008, Wu *et al.* 2009), multivariate regression analysis using classification procedures such as the linear mixture modelling approach (Tyler *et al.* 2006), and the spectral decomposition algorithm (Oyama *et al.* 2007, Oyama *et al.* 2009). Of these, the Neural Network approach has become particularly popular. Neural Networks are essentially a multiple non-linear regression procedure simulating the neural functions of the cerebral cortex of the brain through layers of interacting neurons. The 'input layer' uses the reflectance/radiance in various bands and the 'output layer' gives the concentrations of various parameters or IOPs. The hidden layers consist of neurons which are assigned various weights and bias through training the algorithm with a real or simulated data set of concentrations and reflectances. Neural networks are able to simulate the complex non-linear influence of various parameters on the water leaving reflectance and solve for a variety of parameters simultaneously. For this reason they are also used for analytical algorithms. However, the need for a training data set and problems such as 'over-training' and multiple possible solutions means that these algorithms require substantial effort to implement. Genetic algorithms simulate the process of natural evolution of populations through producing successively 'fitter' generations through processes of selection, cross-over and mutation. These algorithms have a powerful ability to search the full decision space for the optimal solution to linear and non-linear problems but are often combined with procedures such as Neural Networks that improve the precision of the solution (e.g. Wu *et al.* 2009). The use of these and other complex algorithms generally leads to improved significance of correlations, although in some instances the level of complexity of these algorithms does not appear to offer significant enough accuracy improvements to justify their mathematical difficulty.

*4.4 CDOM algorithms.*

CDOM (also called *gelbstoff*, *gilvin* or yellow substances) composed of humic and fulvic acids is a significant contributor to water colour since humic substances absorb strongly in the blue region of the spectrum turning

the water brown. Absorption by CDOM ($a_{CDOM}$), usually referenced at 440 nm, takes on the form of an exponential curve decreasing towards longer wavelengths so that its effects are usually negligible at wavelengths greater than about 550 nm. The slope of the curve is mostly predictable as it varies within a relatively small range (0.10–0.20 $nm^{-1}$) for most inland and coastal waters (Dekker 1993). Absorption by detrital material (organic non-living material of mostly algal origin), mineral and non-pigmented aquatic particles display similar decreasing exponential functions (Babin and Stramski 2002, Babin *et al.* 2003) and can overwhelm the contribution to absorption by CDOM in natural waters if concentrations are high enough. In turn, in situations where $a_{CDOM}$ is very large, i.e. humic lakes, the retrieval of other biogeophysical parameters will also be affected.

The retrieval of $a_{CDOM}$ using remote sensing has been the subject of more recent studies as interest in optical measurements of the inherent optical properties (IOPs) of natural waters is increasing (Lee *et al.* 2002). $a_{CDOM}$ is one of the primary additive absorption IOPs along with phytoplankton and water, and is therefore of great interest from a bio-optical perspective. Since the signal from $a_{CDOM}$ is only significant in the blue region of the spectrum (<550 nm) it serves to reason that the retrieval from remote sensing will utilise suitable bands from this region of the spectrum. An unfortunate consequence of this is that atmospheric scattering is greatest in the blue – and the water-leaving signal so diminished from strong absorption by phytoplankton and CDOM – that the signal from the water may be indistinguishable and the data unusable. This is especially a problem when considering the low radiometric sensitivities of sensors such as Landsat or SPOT. Despite these limitations, there are numerous examples of $a_{CDOM}$ retrieval using both sensitive ocean colour and radiometric sensors, and less sensitive sensors; albeit in some cases with the acceptance of lower correlations.

Algorithms using ratios of reflectance in the blue (~400–500 nm) to that in the green or red (~500–700 nm) have been found to be well correlated with $a_{CDOM}$ (Kutser *et al.* 1998). In waters with low suspended sediment, Bowers *et al.* (2000) showed theoretically, while making some assumptions about particulate absorption, that there is a linear relationship between $a_{CDOM}$ and the ratio of reflectance in the red to the blue. This was confirmed by a small data set (n=8) using the 670/412 nm ratio ($r^2$ = 0.99) and other studies (e.g. Bowers *et al.* 2004). In turbid waters however, this relationship breaks down due to the influence of particulate scattering (Fang *et al.* 2009) and is therefore better described by a nonlinear power-law relationship. Doxaran *et al.* (2005) used a 400/600 nm ratio while D'Sa and Miller (2003) used the SeaWiFS band configurations 412/510, 443/510 and 510/555 nm, all of which gave good results, although this may reflect the existence of strong covariance between Chl *a* and CDOM. Comparable red/blue ratios produced with the MERIS waveband configuration also give similarly strong correlations up to 0.96 (Kallio *et al.* 2001, Ammenberg *et al.* 2002, Koponen *et al.* 2007). Ratios used include MERIS bands 665/490 and 665/550 nm. The use of the 665 nm band takes advantage of the Chl *a* absorption maximum and acts to normalise for the effects of Chl *a* absorption and backscattering by particulate matter. The correlation with the 571–607/607 nm ratio used by Kallio *et al.* (2001), may however be as a result of covariance between TSS and $a_{CDOM}$, and is therefore less likely to be applicable elsewhere as the signal from CDOM at 570 nm is small.

To more effectively discriminate the signal from phytoplankton pigment absorption and that from CDOM in the blue, Gitelson *et al.* (1993) proposed a 'decoding index' difference ratio algorithm to retrieve $a_{CDOM}$ from high resolution radiometric data, where *a* and *b* are regression coefficients:

$$a_{CDOM} = a\left\{\left(R_{480} - \frac{R_{700}}{R_{675}} - R_{520}\right) \div \left(R_{480} + \frac{R_{700}}{R_{675}} + R_{520}\right)\right\}^{b} \quad (m^{-1}) \qquad (4)$$

The 480 nm band is strongly influenced by $a_{CDOM}$, while the band at 520 nm is a reference and the $R_{700}/R_{675}$ ratio a correction factor for Chl *a* absorption. The non-linear power law algorithm gave an $r^2$ value of more than 0.9 for $a_{CDOM}$ at 380 nm in the range 0.1–12 $m^{-1}$ in more than 20 inland water bodies.

Broad-band terrestrial sensors can also be used successfully to estimate $a_{CDOM}$ in lakes and transitional waters, although usually not with the same level of accuracy as with sensitive and high spectral definition instruments. As a result of atmospheric interference, very small signal and influences of Chl *a* absorption, the use of a broad band in the blue (TM1) is limited, or infeasible (Kutser *et al.* 2005b, Kallio *et al.* 2008). Thus CDOM is better estimated taking advantage of its inverse correlation with the band in the green: as CDOM increases, the reflectance in the green gradually decreases (Kutser *et al.* 2005b, Kallio *et al.* 2008). Thus a ratio of the green to red (where influence by CDOM is assumed to be zero) has been shown to be the most useful

algorithm (Kutser *et al.* 2005a, Kutser *et al.* 2009). This may mean that detecting CDOM by terrestrial sensors at low concentrations (<~5 $m^{-1}$ at 440 nm) which does not have a significant impact on reflectance >500 nm is impossible. However, even when using a green/red algorithm with large $a_{CDOM}$, the low radiometric resolution of some sensors makes CDOM estimations infeasible (Kutser *et al.* 2005b). Results show that the minimum acceptable radiometric resolution for mapping CDOM from broad band sensors is about 16-bit – making the TM and IKONOS instruments generally ill suited (Kutser *et al.* 2005b). Nevertheless, successful $a_{CDOM}$ estimations have been given from TM (8 bit) (Kallio *et al.* 2008) and ALI (16 bit) (Kutser *et al.* 2005a, Kutser *et al.* 2005b, Kutser *et al.* 2009) in high CDOM boreal lakes and coastal waters in Finland. These used a nonlinear power law regression of the green/red band ratio to give $r^2$ values <0.84. Using multiple linear regressions Brezonik *et al.* (2005) derived $a_{CDOM}$ from TM with an $r^2$ value of 0.77 for high CDOM lakes in Minnesota.

*4.5 Other parameters algorithms.*

A wide variety of additional parameters have also been retrieved in lakes and near-coastal transitional waters – some of which are included in the studies presented in Table 1. Some of these parameters, such as nutrient concentrations phosphorus or nitrogen, are derived via proxy using their relationship to parameters that are optically-active. These however, are not reviewed here: only parameters that are directly attainable due to their effects on the water-leaving radiance are included. These are, most notably, turbidity , Suspended Particulate Inorganic Matter (SPIM) and phycocyanin (PC) the accessory pigment present in blue-green cyanobacteria.

**4.5.1 Turbidity.** Turbidity is closely related to TSS and $z_{SD}$ measuring either the attenuation of a beam of light passing through water, or more commonly the scattering by particulate matter usually as detected within 90° of the light beam (units = Nephelometric Turbidity Units – NTU). The relationship between TSS and turbidity is variable in space and time owing to variations in particle size distribution, shape, composition and reflective index (Chen *et al.* 2007, Kallio *et al.* 2008). There are numerous recent examples of remote estimation of turbidity from MODIS 250 m (Chen *et al.* 2007, Alcântara *et al.* 2009, Petus *et al.* 2009), Landsat (Lathrop and Lillesand 1986, Vincent *et al.* 2004, Brezonik *et al.* 2005, Wang *et al.* 2006, Kallio *et al.* 2008), other broad band sensors (Lathrop and Lillesand 1989, Hellweger *et al.* 2007, Chen *et al.* 2009) and others (Dierberg and Carriker 1994, Fraser 1998, Koponen *et al.* 2002). As for TSS, algorithms using single bands or ratios in the red are generally most successful owing to the influence of particulate scattering in these bands, provided the impact from phytoplankton pigments is not overwhelming (Kallio *et al.* 2008). Some studies use more advanced spectral unmixing (Alcântara *et al.* 2009) and NN algorithms (Zhang *et al.* 2002).

**4.5.2 The inorganic component of suspended matter.** SPIM may be of interest when large amounts of sediment are entrained in the water column such as in tidal estuaries (e.g. Doxaran *et al.* 2005). Algorithms for SPIM detection are very similar to those for TSS (especially when inorganic matter makes up the majority of TSS) and use red and NIR bands (e.g. Ammenberg *et al.* 2002, Doxaran *et al.* 2005). This is because inorganic particles contribute greatly to scattering in the NIR (Doxaran *et al.* 2007).

**4.5.3 Phycocyanin.** PC is an accessory pigment present in certain species of cyanobacteria. The detection of cyanobacterial *via* phycocyanin is of great interest owing to the potentially great negative impacts these bloom forming and sometimes toxic species have in coastal and inland waters which may result in substantial economic losses. Therefore, an effective means of detecting and monitoring these blooms would be of considerable public value. There have already been numerous attempts to develop an empirical algorithm specifically for detecting PC – there have been other studies aimed at detecting cyanobacterial blooms *via* Chl *a* (e.g. Kutser 2004, Reinart and Kutser 2006). Absorption by PC ~620 nm in turbid cyanobacteria-dominated water results in a distinct minimum in the water leaving reflectance which can potentially be used to detect cyanobacteria specific blooms (Dekker 1993, Jupp *et al.* 1994). Therefore, there should be an inverse relationship between the reflectance near 620 nm and PC concentration – although the influence of water, *tripton*, other phytoplankton pigments and to a lesser extent CDOM can be a significant source of error owing to the relative magnitudes of these absorption coefficients. Furthermore, empirical algorithms exploiting this unique feature ~620 nm require sensors with narrow bands (<12 nm wide – conveniently MERIS has 10 nm wide band centred at 620 nm) and high SNRs (>1000:1) (Dekker 1993, Metsamaa *et al.* 2006). Single bands (~620 nm) and the band ratio 620/650 nm have

been used (Dekker *et al.* 1992, Gitelson *et al.* 1995, Schalles and Yacobi 2000, Ruiz-Verdú *et al.* 2008, Vallely 2008, Mishra *et al.* 2009), but are quite susceptible to errors arising from spectral variations of extraneous parameters. To avoid this problem Dekker *et al.* (1993) subtracted the reflectance at 624 nm from the average of that at 600 and 648 nm as a baseline subtraction and found a strong linear relationship with PC for eutrophic turbid lakes ($r^2 > 0.99$). However, further study shows that the algorithm has a tendency to underestimate and may only be sensitive at concentrations greater than ~10 $mg.m^{-3}$ and less than ~200 $mg.m^{-3}$ as the relationship with the 620 nm reflectance trough is nonlinear outside these ranges (Ruiz-Verdú *et al.* 2008).

Other studies use the 709/620 nm ratio with success (Peña-Martinez *et al.* 2004, Ruiz-Verdú *et al.* 2005, Hunter *et al.* 2008, Hunter *et al.* 2009) or a 700/600 nm ratio (Mishra *et al.* 2009). To account for the complex interactions of absorption by water and Chl *a* (but not CDOM/detritus) Simis *et al.* (2005, 2007)(2007) used a semi-analytical algorithm based on the reflectance approximation (Morel and Prieur 1977) and the 709/620 nm ratio to retrieve the phycocyanin specific absorption coefficient at 620 nm, $a_{pc}(620)$:

$$a_{pc}(620) = \left(\{[R(709)/R(620)][\,a_w(709) + b_b]\} - b_b - a_w(620)\right)\delta^{-1} - [\varepsilon a_{chl}(665)]\ (\mathrm{m}^{-1}) \quad (5)$$

where $a_w$ is the absorption by water, $b_b$ is the spectrally invariant backscattering coefficient, $\delta$ is a correction factor which accounts for the assumption that absorption by CDOM, Chl *a*, and detritus is negligible in the red, $a_{chl}$ is the absorption due to chlorophyll, and $\varepsilon$ is a conversion factor to estimate $a_{chl}$ at 620 nm from that at 665 nm.

The algorithms uses $b_b$ calculated from reflectance at 778 nm according to Gons (1999), and $a_{chl}$ (665) calculated from a very similar semi-analytical algorithm using the 709/665 nm ratio (Simis *et al.* 2005). Final PC concentrations are obtained by dividing $a_{pc}(620)$ by the PC specific absorption coefficient $a^*_{pc}(620)$. This algorithm has been validated by a number of other studies ($r^2$ <0.99) (Simis *et al.* 2007, Randolph *et al.* 2008, Ruiz-Verdú *et al.* 2008, Vallely 2008) and similar semi-analytical algorithms (Yang and Pan 2006). The proven cross-applicability of such an approach makes it potentially very useful for phycocyanin estimations in cyanobacteria dominant eutrophic waters.

As previously discussed, sensors with high spatial resolution, low SNR and wide band widths do not meet the minimum requirements for PC detection. Nonetheless, using Landsat TM and ETM+ Vincent *et al.* (2004) found that multiple linear regressions of band ratios were capable of establishing a correlation with PC ($r^2$<0.78). However, the causality and cross-applicability of such an approach is very limited especially given that the Landsat bands do not overlap the PC absorption maximum at 620 nm. The result is probably explained by a correlation between PC and turbidity or some other parameter (Kutser *et al.* 2006). In general, PC retrieval is best when cyanobacteria form the dominant component of the phytoplankton assemblage due to the confounding effects of other accessory pigments from other phytoplankton groups (Ruiz-Verdú *et al.* 2008). PC estimation from remotely sensed data such as MERIS and new hyperspectral spaceborne sensors (e.g. HICO, Enmap hyperspectral Imager) will likely be used in future to assess cyanobacterial blooms and provide early warning systems (Ahn *et al.* 2007).

**5. Discussion and Conclusion**

Progress towards a bio-optical model-based approach of remote sensing of water has been a necessary advancement of the science of what is now rather inappropriately called ocean colour radiometry (OCR). This shift has been caused by the need for a technique capable of solving the complex signal from mainly coastal waters. Model-based solutions have the ability to simultaneously retrieve various optical and biogeophysical parameters from the remote sensing reflectance. Their theoretical basis on sound solutions to the radiative transfer equation makes them potentially a more expedient approach. So, why write a review focusing on the empirical approach when the science is clearly heading towards model-based approaches? Firstly, there is a growing amount of evidence from recent studies that the empirical approach is more often used than the model based approach and is fully capable of producing reliable estimates of a variety of biogeophysical parameters in inland and transitional waters. Furthermore, the ease of implementation and computational simplicity often makes it the most convenient choice for many water remote sensing studies. These advantages are also favourable for near real-time observation systems, especially where the deployment of autonomous observation

moorings/platforms presents a readily available source of data that can easily be used to parameterise and validate empirical algorithms.

Secondly, empirically-based algorithms have long been used to derive standard products for phytoplankton pigments (Chl *a*) in open-ocean waters, e.g. the SeaWiFS OC4.v4 (O'Reilly *et al.* 1998) or MODIS OC3M (Campbell and Feng 2005) standard algorithms. These algorithms have been parameterised and validated using the great amount of *in situ* data collected with considerable effort over several decades (stored in databases, e.g. the SeaWiFS Bio-Optical Archive and Storage System (SeaBASS) and the NASA bio-optical Marine Algorithm Data set (NOMAD), the new MERIS MAtchup *In-situ* Database (MERMAID)). These empirical algorithms for the open ocean are limited in coastal waters, hence the need for a model-based approach. However, what about empirical algorithms derived specifically for these coastal, inland and transitional waters? Following the review of the large number of studies, the application of empirically-based algorithms to produce common biogeophysical products for inland and transitional waters appears achievable. For example, the 709/664 ratio is remarkably effective for detecting high biomass waters typical of eutrophic/hypertrophic systems (see discussion below). Up until now, only very limited attempts have been made to produce common biogeophysical algorithms in complex coastal waters, lakes or estuaries (e.g. Nechad *et al.* 2003, Gower *et al.* 2005). Parameterisation and validation of such algorithms could be achieved using the great amount of *in situ* data that has been collected in recent years, and will in future be collected from autonomous platforms. This could lead to the development of regionally optical water type specific and perhaps even, for certain applications, global empirically-based algorithms although the latter remains speculative at present.

Thirdly, the bio-optical basis and potential to operate 'independently' of *in situ* data often cited as the main advantages of model-based algorithms is also true for some empirical algorithms. For example, studies such as Bowers *et al.* (2000), Dekker *et al.* (2001, 2002) and Doxaran *et al.* (2006) used bio-optical modelling to derive robust *empirical* algorithms for estimating $a_{CDOM}$, TSS in Dutch lakes, and TSS in the Gironde estuary, France, respectively. These algorithms are in theory able to operate independently from *in situ* data and have the strong theoretical basis of model-based algorithms. There is a need for more studies investigating bio-optical modelling for generating empirical algorithms. It should also be noted that in reality, a great deal *in situ* data on IOPs is required for parameterisation and validation of model-based algorithms if they are to operate reliably on a regional or even local basis. The evidence given above in support of the empirical approach shows that attempts to review and further develop these techniques is justified. Table 3 presents a synthesis of the findings in Section 4.

Table 3 can be used as a guide for selecting appropriate empirical algorithms for use with either broad or narrow band sensors in various inland and transitional waters. It presents suitable detection band(s), band ratios and band arithmetic independent variables for different concentration ranges of the parameters. The explanation of the bio-optical basis establishes a link between the independent variables and the parameter of interest which is important for the cross-applicability and reproducibility of prospective algorithms. From the information in Table 3, empirical algorithms may be created that have a wide range of potential applications for satellite as well as *in situ* sensors. For example, the 700/670 nm ratio algorithm can reliably detect Chl *a* at high concentrations > 30 $mg.m^{-3}$, and could be used to detect the presence of hypertrophic systems. Similarly a NIR ratio algorithm could within reasonable error be used to detect high concentrations of TSS > 30 $g.m^{-3}$, enabling sediment plume monitoring in estuaries. Water clarity ($z_{sd}$) can be determined using a red/blue ratio; the suggested band ratios could be used to detect phycocyanin containing cyanobacterial blooms, albeit with a lesser degree of confidence and depending upon the availability of suitable sensors, to provide warning information to lake managers. Therefore, there are specific applications, e.g. eutrophication assessment, sediment plume monitoring, water clarity assessments etc., for which the empirical approach has a great deal to offer.

Table 3.
Suggested band(s), band ratios, and/or band arithmetic for the detection of water quality parameters in inland and transitional waters using broad band or narrow band sensors based on review of current literature. For details see Section 4.

| Parameter | Sensor spectral resolution | | Bio-optical basis |
|---|---|---|---|
| | Broad bands | Narrow bands (nm) | |
| $z_{SD}$ | Red band or red/blue ratio, e.g. TM3/TM1+TM1. | Red band or blue/red ratio, e.g. 512/620. | Reflectance in red $\propto b_{bp}$. The blue band dominated by $a_\phi$ and $a_{CDOM}$ serves to normalize. |
| TSS | < 10 g.m$^{-3}$: Red/green ratio or (green + red) /2.<br><br>>10 g.m$^{-3}$: Red or NIR band or (green + red) /2.<br><br>>30 g.m$^{-3}$: NIR/red or NIR/green ratio. | <30 g.m$^{-3}$: (560–520)/(560+520) or single red band, e.g. 700.<br><br>>30 g.m$^{-3}$: NIR ratio, e.g. 850/550. | The $a_\phi$ minimum at 560 nm is sensitive to TSS while the 520 nm band serves to normalize.<br><br>Reflectance in red and NIR $\propto b_{bp}$ and $b_{bm}$. Band ratios normalize for variations in particle refractive indices and grain sizes. |
| Chl *a* | <20 mg.m$^{-3}$: Green/blue ratio or (blue-red)/green.<br><br>>20 mg.m$^{-3}$: Red/blue or red/NIR ratio. | <30 mg.m$^{-3}$: 560 or FLH algorithm.<br><br>>30 mg.m$^{-3}$: 700/670 ratio or 'three band model' 750(1/670–1/710) or RLH or SUM algorithms. | Chl *a* $\propto$ reflectance in red due to $b_{bp}$, and inversely related to reflectance in blue due to $a_\phi$.<br><br>Reflectance at 700 nm sensitive to $b_{b\phi}$ normalized by the $a_\phi$ maximum near 665 nm. |
| $a_{CDOM}$ | Green/red ratio. | Red/blue ratio, e.g. 670/412, or 'decoding index', (490– (700/675)–520)/ (490+(700/675)+520). | Relatively insensitive sensors: Reflectance in green inversely related to $a_{CDOM}$ normalized by reflectance in red.<br><br>Sensitive sensors: Reflectance in blue inversely related to $a_{CDOM}$ normalized by the reflectance in the red. |
| Turbidity | Red band. | Red or NIR band. | Reflectance in red and NIR $\propto b_{bp}$ and $b_{bm}$. |
| SPIM | Red or NIR band. | Red or NIR band. | Reflectance in red and NIR $\propto b_{bp}$ and $b_{bm}$. |
| PC | - | 620/650 or 709/620 ratio or (600+648)/2 –624. | Reflectance at 620 nm inversely related to PC due to absorption maximum. |

A certain degree of error will inevitably be associated with any estimates from remote sensing: nevertheless an acceptable level of error should be determined using sensitivity analyses or *in situ* validation. The size of the error will depend upon the magnitude of the signal from the parameter (large=less error, small=greater error), instrumental design (hyperspectral/broad band, SNR), the data quality (e.g., atmospheric correction if used), and the degree to which the algorithm is parameterised for the system under investigation. With current instrumental constraints, and allowing for the complexity of detection, it is important to recognise that certain parameters such as $a_{CDOM}$ and PC can be estimated with less confidence than others. Targets with smaller signals, such as clear-water oligotrophic systems, will also remain more challenging than systems with larger signals, e.g., hypertrophic or sediment laden waters. The error associated with estimates means that in some instances the information could be viewed as qualitative rather than explicitly quantitative, although quantitatively accurate estimates are desirable. Thus, while accepting a certain degree of error which remains to be determined, a great amount of useful information is readily accessible using the empirical approach.

Global assessments of the quality, quantity and changes occurring in inland fresh and transitional waters from remote sensing are likely to become commonplace within the next few decades. Remote sensing will play a vital role in determining the growing impact that global change will have on these limited and increasingly valuable resources. The achievement of this goal will depend upon the availability of suitable techniques capable of providing reliable information on a regional and possibly even larger scale. This might be realized through moving towards the development not only of model-based algorithms, but also of empirically-based algorithms for common use in inland and transitional waters. The empirical approach, which is easy to implement and computational simple, could play an important role alongside more advanced modelling procedures in the future of water remote sensing, especially for operational near real-time water observation systems. As satellite sensors become more advanced in terms of spectral resolution, sensitivity and frequency of acquisition (even geostationary orbits), the detection of various parameters should improve providing a wealth of information for water quality monitoring and assessment. A number of outstanding issues still need to be addressed with regard to empirical algorithms. There is a need for cooperative parameterisation and validation of empirical algorithms facilitated by a collective database containing *in situ* measurements in inland and transitional waters. Error assessment and sensitivity analyses should also be performed as part of this process to gain estimates of the accuracy and precision of the algorithms. Finally, large quantities of archived data from sensors such as MODIS and MERIS containing a wealth of potential information on inland and transitional waters have yet to be processed.

This paper has provided a review of current empirical methods of retrieving various biogeophysical and optical parameters from remotely sensed data in inland and transitional waters. It provides an overview of the optimal current empirical procedures for estimating these parameters in a diversity of inland and coastal waters from a variety of remotely sensed instruments mounted on *in situ*, airborne and satellite platforms. Importantly, the review has not included more advanced inverse radiative transfer modelling or inversion algorithms, and readers are encouraged to find these elsewhere (e.g. IOCCG 2000, IOCCG 2006). The review demonstrates the considerable number of recent studies using empirical procedures and the continual rapidly growing interest in water remote sensing. Therefore, although trends in bio-optical remote sensing point towards the use of more advanced inversion type models based on radiative transfer which offer a suite of simultaneously derived optical and biogeophysical products (e.g. Odermatt *et al.* 2008), the usefulness of simpler yet robust empirical procedures is palpable. In operational monitoring contexts the empirical approach has a demonstrable capability to provide timely and accurate information for a variety of parameters in lakes and estuaries that can be used for a diversity of applications. Current and future spaceborne remote sensing instruments have also been reviewed. It is hoped that the review will provide a useful reference for workers seeking to employ empirical procedures of remote sensing in inland and transitional Case 2 waters.

## 6. Acknowledgements

The University of Cape Town Postgraduate Publication Incentives Scholarship, one anonymous reviewer for their useful comments and criticisms, my supervisor Dr. Stewart Bernard for encouraging me to write this paper.

## 7. Appendix A. List of abbreviations in Table 1.

| **Data type** |
|---|
| AISA = Airborne Imaging Spectrometer for Applications |
| ALI = Advanced Land Imager |
| AMMS = Airborne Multispectral Measurement System |
| ASTER = Advances Spaceborne Thermal Emission and Reflection Radiometer |
| CASI = Compact Airborne Spectrographic Imager |
| CHRIS = Compact High Resolution Imaging Spectrometer |
| DS-1260 MSS = Airborne Daedalus Multi Spectral Scanner |
| LS 7 ETM+ = Landsat 7 Enhanced Thematic Mapper |
| LS TM = Landsat Thematic Mapper |
| LISS III = Linear Imaging Self-Scanning Sensor |
| MERIS = Medium Resolution Imaging Spectrometer |
| MIVIS = Multispectral Infrared and Visible Imaging Spectrometer |
| MODIS = Moderate Resolution Imaging Spectrometer |
| ROSIS = Reflective Optics System Imaging Spectrometer |
| SeaWiFS = Sea-viewing Wide Field-of-view Sensor |
| SEVERI MSG = Spinning Enhanced Visible and InfraRed Imager on METEOSAT Second Generation |
| Spec. = Spectroradiometer |
| SPOT HRV = Le Systeme Pour l'Observation de la Terra High Resolution Visible |
| **Water Quality Parameters (WQPs)** |
| $a_{CDOM}$ = absorption by Coloured Dissolved Organic Matter |
| BOD = Biological Oxygen Demand |
| Chl *a* = Chlorophyll *a* |
| COD = Chemical Oxygen Demand |
| PC = Phycocyanin pigment |
| $z_{SD}$ = Secchi Disk depth |
| SPIM = Suspended Particulate Inorganic Material |
| TOC = Total Organic Carbon |
| TSS = Total Suspended Solids |
| Turb = Turbidity |
| **Atmospheric correction** |
| 6S = Second Simulation of the Satellite Signal in the Solar Spectrum (Vermote *et al*., 1997) |
| DDV = Dense Dark Vegetation |
| DOS = Dark Object Subtraction |
| ELM = Empirical Line Method (Moran *et al*., 2001) |
| LOWTRAN = Low Resolution Atmospheric Transmittance Code |
| MODTRAN = Moderate Resolution Atmospheric Transmittance Code |
| MUMM = Management Unit of the North Sea Mathematical Models |
| RTC = Radiative Transfer Code |
| SMAC = Simplified Method of Atmospheric Correction (Rahman and Dedieu 1994) |
| SOS = Successive Order of Scattering Code (Lenoble *et al.* 2007) |
| **Statistical technique** |
| ANN = Artificial Neural Network |
| BOM =Bio-Optical Model |

| |
|---|
| CHROM = Chromaticity analysis |
| GEGA = Grammatical Evolution Genetic Algorithm |
| LMM = Linear Mixture Modelling |
| LR = Linear Regression |
| LSU = Linear Spectral Unmixing |
| LT-LR = Log-Transformed Linear Regression |
| LT-MLR = Log-Transformed Multiple Linear Regression |
| LT-MLSR = Log-Transformed Multiple Linear Stepwise Regression |
| MIP = Modular Inversion and Processing System |
| MLR = Multiple Linear Regression |
| MLSR = Multiple Linear Stepwise Regression |
| NLR =Non-Linear Regression |
| Poly = Polynomial regression (number indicated order) |
| PCA = Principal Component Analysis |
| SA = Semi-analytical |
| SAM = Spectral Angle Mapper |
| SDA = Spectral Decomposition Algorithm |
| UC = Unsupervised Classification |

**8. References.**


AHN, C.Y., JOUNG, S.H., YOON, S.K., and OH, H.M., 2007, Alternative Alert System for Cyanobacterial Bloom, Using Phycocyanin as a Level Determinant. *The Journal of Microbiology,* **45**, pp. 98-104.

ALCÂNTARA, E., BARBOSA, C., STECH, J., NOVO, E., and SHIMABUKURO, Y., 2009, Improving the spectral unmixing algorithm to map water turbidity Distributions. *Environmental Modelling and Software*, **24**, pp. 1051-1061.

ALPARSLAN, E., AYDONER, C., TUFEKCI, V., and TUFEKCI, H., 2007, Water quality assessment at Omerli Dam using remote sensing techniques. *Environmental Monitoring and Assessment,* **135**, pp. 391-398.

AL-SAADI, J. A., K. W. JUCKS, P. S. BONTEMPI, E. HILSENRATH, L. T. IRACI, J. W. CAMPBELL, J. FISHMAN, S. R. KAWA, and A. MANNINO, 2009, The NASA GEO-CAPE Mission. In *American Geophysical Union Fall Meeting, 14-18 December 2009, abstract #A51M-02,* San Francisco, CA (Published online: AGU) pp. 02.

AMMENBERG, P., FLINK, P., LINDELL, T., PIERSON, D., and STROMBECK, N., 2002, Bio-optical modelling combined with remote sensing to assess water quality. *International Journal of Remote Sensing,* **23**, pp. 1621-1638.

BABIN, M., and STRAMSKI, D., 2002, Light absorption by aquatic particles in the near-infrared spectral region. *Limnology and Oceanography,* **47**, pp. 911-915.

BABIN, M., STRAMSKI, D., FERRARI, G.M., CLAUSTRE, H., BRICAUD, A., OBOLENSKY, G., and HOEPFFNER, N., 2003, Variations in the light absorption coefficients of phytoplankton, nonalgal particles, and dissolved organic matter in coastal waters around Europe. *Journal of Geophysical Research,* **108**, pp. 3211-3230.

BOWERS, D., EVANS, D., THOMAS, D., ELLIS, K., and WILLIAMS, P.J.B., 2004, Interpreting the colour of an estuary. *Estuarine, Coastal and Shelf Science,* **59**, pp. 13-20.

BOWERS, D., HARKER, G., SMITH, P., and TETT, P., 2000, Optical properties of a region of freshwater influence (the Clyde Sea). *Estuarine, Coastal and Shelf Science,* **50**, pp. 717-726.

BRANDO, V.E., and DEKKER, A.G., 2003, Satellite hyperspectral remote sensing for estimating estuarine and coastal water quality. *IEEE Transactions on Geoscience and Remote Sensing,* **41**, pp. 1378-1387.

BREZONIK, P., MENKEN, K.D., and BAUER, M., 2005, Landsat-based remote sensing of lake water quality characteristics, including chlorophyll and Colored Dissolved Organic Matter(CDOM). *Lake and Reservoir Management,* **21**, pp. 373-382.

BRIVIO, P.A., GIARDINO, C., and ZILIOLI, E., 2001, Determination of chlorophyll concentration changes in Lake Garda using an image-based radiative transfer code for Landsat TM images. *International Journal of Remote Sensing,* **22**, pp. 487-502.

BUITEVELD, H., J. H. M. HAKVOORT, and M. DONZE, 1994, Optical properties of pure water. In *Proceedings of SPIE, Ocean Optics XII,* Bergen, Norway (Published online: SPIE) pp. 174-183.

CAMPBELL, J. W., and H. FENG, 2005, The empirical chlorophyll algorithm for MODIS: Testing the OC3M algorithm using NOMAD data. In *Ocean Color Bio-optical Algorithm Mini-workshop, 27 - 29 September 2005,* New England Center, University of New Hampshire (Durham, New Hampshire: NASA) pp. 1-9.

CANDIANI, G., D. FLORICIOIU, C. GIARDINO, and H. ROTT, 2005, Monitoring water quality of the perialpine Ilalian Lake Guarda through multi-temporal MERIS data. In *Proceedings of the MERIS (A)ATSR Workshop, Frascati, Italy 26 - 30 Spetember 2005,* (Published on CDROM: ESA) pp. 1.

CHANG, K.W., SHEN, Y., and CHEN, P.C., 2004, Predicting algal bloom in the Techi reservoir using Landsat TM data. *International Journal of Remote Sensing,* **25**, pp. 3411-3422.

CHAVULA, G., BREZONIK, P., THENKABAIL, P., JOHNSON, T., and BAUER, M., 2009, Estimating chlorophyll concentration in Lake Malawi from MODIS satellite imagery. *Physics and Chemistry of the Earth,* **34**, pp. 755-760.

CHEN, S., FANG, L., ZHANG, L., and HUANG, W., 2009, Remote sensing of turbidity in seawater intrusion reaches of Pearl River Estuary–A case study in Modaomen water way, China. *Estuarine, Coastal and Shelf Science*, **82**, pp. 119-127.

CHEN, L., TAN, C.H., KAO, S.J., and WANG, T.S., 2008, Improvement of remote monitoring on water quality in a subtropical reservoir by incorporating grammatical evolution with parallel genetic algorithms into satellite imagery. *Water research,* **42**, pp. 296-306.

CHEN, Z., HU, C., and MULLER-KARGER, F., 2007, Monitoring turbidity in Tampa Bay using MODIS/Aqua 250-m imagery. *Remote Sensing of Environment,* **109**, pp. 207-220.

CORSON, M. R., D. R. KORWAN, R. L. LUCKE, W. A. SNYDER, and C. O. DAVIS, 2008, The Hyperspectral Imager for the Coastal Ocean (HICO) on the International Space Station. In *IEEE International Geoscience and Remote Sensing Symposium, 2008,* Boston, Massachusetts, U.S.A (Published online: IEEE) pp. TH1.109.

COX, R.M., FORSYTHE, R.D., VAUGHAN, G.E., and OLMSTED, L.L., 1998, Assessing water quality in Catawba River reservoirs using Landsat Thematic Mapper satellite data. *Lake and Reservoir Management,* **14**, pp. 405-416.

DALL'OLMO, G., and GITELSON, A.A., 2005, Effect of bio-optical parameter variability on the remote estimation of chlorophyll-a concentration in turbid productive waters: experimental results. *Applied Optics*, **44**, pp. 412-422.

DEFOIN-PLATEL, M., and CHAMI, M., 2007, How ambiguous is the inverse problem of ocean color in coastal waters? *Journal of Geophysical Research,* **112**, pp. C03004.1-C03004.16.

DEKKER, A., 1993, Detection of optical water quality parameters for eutrophic waters by high resolution remote sensing. Ph.D. thesis, Free University, Amsterdam.

DEKKER, A. G., T. J. MALTHUS, and L. M. GODDIJN, 1992, Monitoring cyanobacteria in eutrophic waters using airborne imaging spectroscopy and multispectral remote sensing systems. In *Proc. 6th Australasian Remote Sensing Conference, 2-6 November 1992*, Wellington, New Zealand (New Zealand: Committee of the conference) pp. 204-214.

DEKKER, A.G., VOS, R.J., and PETERS, S.W.M., 2002, Analytical algorithms for lake water TSM estimation for retrospective analyses of TM and SPOT sensor data. *International Journal of Remote Sensing*, **23**, pp. 15-35.

DEKKER, A.G., VOS, R.J., and PETERS, S.W.M., 2001, Comparison of remote sensing data, model results and in situ data for total suspended matter (TSM) in the southern Frisian lakes. *Science of the Total Environment,* **268**, pp. 197-214.

DIERBERG, F.E., and CARRIKER, N.E., 1994, Field testing two instruments for remotely sensing water quality in the Tennessee Valley. *Environmental science & technology,* **28**, pp. 16-25.

DOERFFER, R., and H. SCHILLER, 2008a, MERIS lake water algorithm for BEAM Algorithm Theoretical Basis Document (ATBD). No. 1.0, 1-17 pp.

DOERFFER, R., and H. SCHILLER, 2008b, MERIS regional coastal and lake case 2 water project - atmospheric correction Algorithm Theoretical Basis Document (ATBD). No. 1.0, 1-42 pp.

DOR, I., and BEN-YOSEF, N., 1996, Monitoring effluent quality in hypertrophic wastewater reservoirs using remote sensing. *Water Science and Technology,* **33**, pp. 23-29.

DOXARAN, D., BABIN, M., and LEYMARIE, E., 2007, Near-infrared light scattering by particles in coastal waters. *Optics Express,* **15**, pp. 12834-12849.

DOXARAN, D., CASTAING, P., and LAVENDER, S., 2006, Monitoring the maximum turbidity zone and detecting finescale turbidity features in the Gironde estuary using high spatial resolution satellite sensor (SPOT HRV, Landsat ETM ) data. *International Journal of Remote Sensing,* **27**, pp. 2303-2321.

DOXARAN, D., CHERUKURU, R., and LAVENDER, S., 2005, Use of reflectance band ratios to estimate suspended and dissolved matter concentrations in estuarine waters. *International Journal of Remote Sensing,* **26**, pp. 1763-1770.

DOXARAN, D., FROIDEFOND, J.M., and CASTAING, P., 2003, Remote-sensing reflectance of turbid sediment-dominated waters. Reduction of sediment type variations and changing illumination conditions effects by use of reflectance ratios. *Applied Optics,* **42**, pp. 2623-2634.

DOXARAN, D., FROIDEFOND, J.M., and CASTAING, P., 2002, A reflectance band ratio used to estimate suspended matter concentrations in sediment-dominated coastal waters. *International Journal of Remote Sensing,* **23**, pp. 5079-5085.

DOXARAN, D., FROIDEFOND, J.M., CASTAING, P., and BABIN, M., 2009, Dynamics of the turbidity maximum zone in a macrotidal estuary (the Gironde, France): Observations from field and MODIS satellite data. *Estuarine, Coastal and Shelf Science,* **81**, pp. 321-332.

DOXARAN, D., FROIDEFOND, J.M., LAVENDER, S., and CASTAING, P., 2002, Spectral signature of highly turbid waters: Application with SPOT data to quantify suspended particulate matter concentrations. *Remote Sensing of Environment,* **81**, pp. 149-161.

D'SA, E.J., and MILLER, R.L., 2003, Bio-optical properties in waters influenced by the Mississippi River during low flow conditions. *Remote Sensing of Environment,* **84**, pp. 538-549.

DUAN, H., MA, R., ZHANG, Y., and ZHANG, B., 2009, Remote-sensing assessment of regional inland lake water clarity in northeast China. *Limnology,* **10**, pp. 135-141.

DUAN, H.T., ZHANG, Y.Z., ZHAN, B., SONG, K.S., and WANG, Z.M., 2007, Assessment of chlorophyll-a concentration and trophic state for Lake Chagan using Landsat TM and field spectral data. *Environmental Monitoring and Assessment,* **129**, pp. 295-308.

DURAND, D., D. V. POZDNYAKOV, S. SANDVEN, F. CAUNEAU, L. WALD, A. JACOB, K. KLOSTER, and M. MILES, 1999, Characterisation of inland and coastal waters with space sensors: final report. Technical report No. 164, 1-180 pp.

FANG, L.G., CHEN, S.S., LI, D., and LI, H.L., 2009, Use of Reflectance Ratios as a Proxy for Coastal Water Constituent Monitoring in the Pearl River Estuary. *Sensors,* **9**, pp. 656-673.

FLINK, P., LINDELL, T., and ÖSTLUND, C., 2001, Statistical analysis of hyperspectral data from two Swedish lakes. *The Science of the Total Environment,* **268**, pp. 155-169.

FLORICIOIU, D., C. RIEDL, H. ROTT, and E. ROTT, 2003, Envisat MERIS capabilities for monitoring the water quality of perialpine lakes. In *Proceedings of IEEE Geoscience and Remote Sensing Symposium, 21-25 July 2003, Toulouse, France,* (published on CDROM: IEEE IGARSS 2003) pp. 2134-2136.

FLORICIOIU, D., H. ROTT, E. ROTT, M. DOKULIL, and C. DEFRANCESCO, 2004, Retrieval of limnological parameters of perialpine lakes by means of MERIS data. In *Proceedings of the 2004 Envisat & ERS Symposium (ESA SP-572), 6 - 10 September,* Salzberg, Austria (Published on CDROM: ESRIN-ESA) pp. 1-5.

FRASER, R.N., 1998, Hyperspectral remote sensing of turbidity and chlorophyll a among Nebraska Sand Hills lakes. *International Journal of Remote Sensing,* **19**, pp. 1579-1589.

FRASER, R.S., FERRARE, R.A., KAUFMAN, Y.J., MARKHAM, B.L., and MATTOO, S., 1992, Algorithm for atmospheric corrections of aircraft and satellite imagery. *International Journal of Remote Sensing,* **13**, pp. 541-557.

GEGE, P., 1998, Characterization of the phytoplankton in Lake Constance for classification by remote sensing. *Archiv fuer Hydrobiologie-Special Issues Advancements in Limnology,* **53**, pp. 179–193.

GIARDINO, C., BRANDO, V.E., DEKKER, A.G., STRÖMBECK, N., and CANDIANI, G., 2007, Assessment of water quality in Lake Garda (Italy) using Hyperion. *Remote Sensing of Environment,* **109**, pp. 183-195.

GIARDINO, C., CANDIANI, G., and ZILIOLI, E., 2005, Detecting chlorophyll-a in Lake Guarda using TOA MERIS radiances. *Photogrammetric Engineering & Remote Sensing,* **71**, pp. 1045-1051.

GIARDINO, C., PEPE, M., BRIVIO, P.A., GHEZZI, P., and ZILIOLI, E., 2001, Detecting chlorophyll, Secchi disk depth and surface temperature in a sub-alpine lake using Landsat imagery. *The Science of the Total Environment,* **268**, pp. 19-29.

GITELSON, A., 1992, The peak near 700 nm on radiance spectra of algae and water: relationships of its magnitude and position with chlorophyll concentration. *International Journal of Remote Sensing,* **13**, pp. 3367-3373.

GITELSON, A., GARBUZOV, G., SZILAGYI, F., MITTENZWEY, K., KARNIELI, A., and KAISER, A., 1993, Quantitative remote sensing methods for real-time monitoring of inland waters quality. *International Journal of Remote Sensing,* **14**, pp. 1269-1295.

GITELSON, A., MAYO, M., YACOBI, Y.Z., PARPAROV, A., and BERMAN, T., 1994, The use of high-spectral-resolution radiometer data for detection of low chlorophyll concentrations in Lake Kinneret. *Journal of Plankton Research,* **16**, pp. 993-1002.

GITELSON, A.A., DALL'OLMO, G., MOSES, W., RUNDQUIST, D.C., BARROW, T., FISHER, T.R., GURLIN, D., and HOLZ, J., 2008, A simple semi-analytical model for remote estimation of chlorophyll-a in turbid waters: validation. *Remote Sensing of Environment,* **112**, pp. 3582-3593.

GITELSON, A.A., GRITZ, Y., and MERZLYAK, M.N., 2003, Relationships between leaf chlorophyll content and spectral reflectance and algorithms for non-destructive chlorophyll assessment in higher plant leaves. *Journal of Plant Physiology,* **160**, pp. 271-282.

GITELSON, A.A., GURLIN, D., MOSES, W.J., and BARROW, T., 2009, A bio-optical algorithm for the remote estimation of the chlorophyll-a concentration in case 2 waters. *Environmental Research Letters,* **4**, pp. 045003.

GITELSON, A.A., LAORAWAT, S., KEYDAN, G.P., and VONSHAK, A., 1995, Optical properties of dense algal cultures outdoors and their application to remote estimation of biomass and pigment concentration in Spirulina platensis (Cyanobacteria). *Journal of Phycology,* **31**, pp. 828-834.

GITELSON, A.A., YACOBI, Y.Z., KARNIELI, A., and KRESS, N., 1996, Reflectance spectra of polluted marine waters in Haifa Bay, Southeastern Mediterranean: features and application for remote estimation of chlorophyll concentration. *Israel Journal of Earth Science,* **45**, pp. 127-136.

GLASGOW, H.B., BURKHOLDER, J.M., REED, R.E., LEWITUS, A.J., and KLEINMAN, J.E., 2004, Real-time remote monitoring of water quality: a review of current applications, and advancements in sensor, telemetry, and computing technologies. *Journal of experimental marine biology and ecology,* **300**, pp. 409-448.

GONS, H.J., 1999, Optical teledetection of chlorophyll *a* in turbid inland waters. *Environmental science & technology,* **33**, pp. 1127-1132.

GONS, H.J., RIJKEBOER, M., and RUDDICK, K.G., 2005, Effect of a waveband shift on chlorophyll retrieval from MERIS imagery of inland and coastal waters. *Journal of Plankton Research,* **27**, pp. 125-127.

GONS, H.J., RIJKEBOER, M., and RUDDICK, K.G., 2002, A chlorophyll-retrieval algorithm for satellite imagery (Medium Resolution Imaging Spectrometer) of inland and coastal waters. *Journal of Plankton Research,* **24**, pp. 947-951.

GOWER, J., KING, S., BORSTAD, G., and BROWN, L., 2005, Detection of intense plankton blooms using the 709 nm band of the MERIS imaging spectrometer. *International Journal of Remote Sensing,* **26**, pp. 2005-2012.

GOWER, J.F.R., DOERFFER, R., and BORSTAD, G.A., 1999, Interpretation of the 685nm peak in water-leaving radiance spectra in terms of fluorescence, absorption and scattering, and its observation by MERIS. *International Journal of Remote Sensing,* **20**, pp. 1771-1786.

GOWER, J., 1980, Observations of in situ fluorescence of chlorophyll-a in Saanich Inlet. *Boundary-Layer Meteorology,* **18**, pp. 235-245.

HAKVOORT, H., DE HAAN, J., JORDANS, R., VOS, R., PETERS, S., and RIJKEBOER, M., 2002, Towards airborne remote sensing of water quality in The Netherlands—validation and error analysis. *ISPRS Journal of Photogrammetry and Remote Sensing,* **57**, pp. 171-183.

HAN, L., and JORDAN, K., 2005, Estimating and mapping chlorophyll a concentration in Pensacola Bay, Florida using Landsat ETM data. *International Journal of Remote Sensing,* **26**, pp. 5245-5254.

HÄRMÄ, P., VEPSALAINEN, J., HANNONEN, T., PYHALAHTI, T., KAMARI, J., KALLIO, K., ELOHEIMO, K., and KOPONEN, S., 2001, Detection of water quality using simulated satellite data and semi-empirical algorithms in Finland. *The Science of the Total Environment,* **268**, pp. 107-121.

HELLWEGER, F.L., SCHLOSSER, P., LALL, U., and WEISSEL, J.K., 2004, Use of satellite imagery for water quality studies in New York Harbor. *Estuarine, Coastal and Shelf Science,* **61**, pp. 437-448.

HELLWEGER, F.L., MILLER, W., and OSHODI, K.S., 2007, Mapping turbidity in the Charles River, Boston using a high-resolution satellite. *Environmental Monitoring and Assessment,* **132**, pp. 311-320.

HUNTER, P., TYLER, A.N., WILLBY, N.J., and GILVEAR, D.J., 2008, The spatial dynamics of vertical migration by Microcystis aeruginosa in a eutrophic shallow lake: A case study using high spatial resolution time- series airborne remote sensing. *Limnology and Oceanography,* **53**, pp. 2391-2406.

HUNTER, P.D., TYLER, A.N., GILVEAR, D.J., and WILLBY, N.J., 2009, Using Remote Sensing to Aid the Assessment of Human Health Risks from Blooms of Potentially Toxic Cyanobacteria. *Environmental Science and Technology,* **43**, pp. 2627-2633.

HUNTER, P.D., TYLER, A.N., PRÉSING, M., KOVÁCS, A.W., and PRESTON, T., 2008, Spectral discrimination of phytoplankton colour groups: The effect of suspended particulate matter and sensor spectral resolution. *Remote Sensing of Environment,* **112**, pp. 1527-1544.

IOCCG, 2006, Remote sensing of inherent optical properties: Fundamentals, tests of algorithms, and applications. Reports of the International Ocean-Colour Coordinating Group, No. 5, 1-126 pp.

IOCCG, 2000, Remote sensing of ocean colour in coastal, and other optically-complex, waters. Reports of the International Ocean-Colour Coordinating Group, No. 3, 1-140 pp.

JIAO, H.B., ZHA, Y., GAO, J., LI, Y.M., WEI, Y.C., and HUANG, J.Z., 2006, Estimation of chlorophyll a concentration in Lake Tai, China using in situ hyperspectral data. *International Journal of Remote Sensing,* **27**, pp. 4267-4276.

JUPP, D.L.B., KIRK, J.T.O., and HARRIS, G.P., 1994, Detection, identification and mapping of cyanobacteria-- Using remote sensing to measure the optical quality of turbid inland waters. *Australian Journal of Marine and Freshwater Research,* **45**, pp. 801-828.

KALLIO, K., ATTILA, J., HÄRMÄ, P., KOPONEN, S., PULLIAINEN, J., HYYTIÄINEN, U.M., and PYHÄLAHTI, T., 2008, Landsat ETM Images in the Estimation of Seasonal Lake Water Quality in Boreal River Basins. *Environmental management,* **42**, pp. 511-522.

KALLIO, K., KOPONEN, S., and PULLIAINEN, J., 2003, Feasibility of airborne imaging spectrometry for lake monitoring—a case study of spatial chlorophyll a distribution in two meso-eutrophic lakes. *International Journal of Remote Sensing,* **24**, pp. 3771-3790.

KALLIO, K., KUTSER, T., HANNONEN, T., KOPONEN, S., PULLIAINEN, J., VEPSALAINEN, J., and PYHALAHTI, T., 2001, Retrieval of water quality from airborne imaging spectrometry of various lake types in different seasons. *The Science of the Total Environment,* **268**, pp. 59-77.

KANG, G., H. S. YOUN, S. B. CHOI, and P. COSTE, 2006, Radiometric calibration of COMS geostationary ocean color imager. In *Proceedings of SPIE,* Stockholm, Sweden (Published online: SPIE) pp. 636112.

KIRK, J. T. O., 1994, *Light and photosynthesis in aquatic ecosystems,* pp. 509 (Bristol: Cambridge University Press).

KLOIBER, S.M., BREZONIK, P.L., OLMANSON, L.G., and BAUER, M.E., 2002, A procedure for regional lake water clarity assessment using Landsat multispectral data. *Remote Sensing of Environment,* **82**, pp. 38-47.

KNEIZYS, F.X., E.P. SHETTLE, L.W. ABREU, J.H. CHETWYND, G.P. ANDERSON, W.O. GALLERY, J.E.A. SELBY, and S.A. CLOUGH, 1988, Users guide to LOWTRAN 7. Environmental Research Report (ERP) No. 1010, 1-148 pp.

KOPONEN, S., ATTILA, J., PULLIAINEN, J., KALLIO, K., PYHÄLAHTI, T., LINDFORS, A., RASMUS, K., and HALLIKAINEN, M., 2007, A case study of airborne and satellite remote sensing of a spring bloom event in the Gulf of Finland. *Continental Shelf Research,* **27**, pp. 228-244.

KOPONEN, S., KALLIO, K., PULLIAINEN, J., VEPSALAINEN, J., PYHALAHTI, T., and HALLIKAINEN, M., 2004, Water quality classification of lakes using 250-m MODIS data. *Geoscience and Remote Sensing Letters, IEEE,* **1**, pp. 287-291.

KOPONEN, S., PULLIAINEN, J., KALLIO, K., and HALLIKAINEN, M., 2002, Lake water quality classification with airborne hyperspectral spectrometer and simulated MERIS data. *Remote Sensing of Environment,* **79**, pp. 51-59.

KRATZER, S., BROCKMANN, C., and MOORE, G., 2008, Using MERIS full resolution data to monitor coastal waters—A case study from Himmerfjärden, a fjord-like bay in the northwestern Baltic Sea. *Remote Sensing of Environment,* **112**, pp. 2284-2300.

KUTSER, T., 2009, Passive optical remote sensing of cyanobacteria and other intense phytoplankton blooms in coastal and inland waters. *International Journal of Remote Sensing,* **30**, pp. 4401-4425.

KUTSER, T., 2004, Quantitative detection of chlorophyll in cyanobacterial blooms by satellite remote sensing. *Limnology and Oceanography,* **49**, pp. 2179-2189.

KUTSER, T., ARST, H., MÄEKIVI, S., and KALLASTE, K., 1998, Estimation of the water quality of the Baltic Sea and lakes in Estonia and Finland by passive optical remote sensing measurements on board vessel. *Lakes & Reservoirs: Research and Management,* **3**, pp. 53-66.

KUTSER, T., METSAMAA, L., STRÖMBECK, N., and VAHTMÄE, E., 2006, Monitoring cyanobacterial blooms by satellite remote sensing. *Estuarine, Coastal and Shelf Science,* **67**, pp. 303-312.

KUTSER, T., PAAVEL, B., and METSAMAA, L., 2009, Mapping coloured dissolved organic matter concentration in coastal waters. *International Journal of Remote Sensing,* **30**, pp. 5843-5849.

KUTSER, T., PIERSON, D.C., KALLIO, K.Y., REINART, A., and SOBEK, S., 2005a, Mapping lake CDOM by satellite remote sensing. *Remote Sensing of Environment*, **94**, pp. 535-540.

KUTSER, T., PIERSON, D., TRANVIK, L., REINART, A., SOBEK, S., and KALLIO, K., 2005b, Using satellite remote sensing to estimate the colored dissolved organic matter absorption coefficient in lakes. *Ecosystems*, **8**, pp. 709-720.

LATHROP, R.G., and LILLESAND, T.M., 1989, Monitoring water quality and river plume transport in Green Bay, Lake Michigan with SPOT-1 imagery. *Photogrammetric Engineering and Remote Sensing*, **55**, pp. 349-354.

LATHROP, R.G., and LILLESAND, T.M., 1986, Use of thematic mapper data to assess water quality in Green Bay and Central Lake Michigan. *Photogrammetric Engineering and Remote Sensing*, **52**, pp. 671-680.

LATHROP, R., 1992, Landsat Thematic Mapper monitoring of turbid inland water quality. *Photogrammetric Engineering and Remote Sensing*, **58**, pp. 465-470.

LAVERY, P., PATTIARATCHI, C., WYLLIE, A., and HICK, P., 1993, Water quality monitoring in estuarine waters using the Landsat Thematic Mapper. *Remote Sensing of Environment*, **46**, pp. 268-280.

LE NAOUR, C., G. EICHEN, and J. F. LÉON, 2006, OCAPI: A Multidirectional Multichannel Polarizing Imager. In *Proceedings of the 6th International Conference on Space Optics, ESTEC, 27-30 June 2006*, Noordwijk, The Netherlands (Netherlands: ESA SP-621) pp. 175-180.

LE, C., LI, Y., ZHA, Y., SUN, D., HUANG, C., and LU, H., 2009, A four-band semi-analytical model for estimating chlorophyll a in highly turbid lakes: The case of Taihu Lake, China. *Remote Sensing of Environment*, **113**, pp. 1175-1182.

LEE, Z.P., CARDER, K.L., and ARNONE, R.A., 2002, Deriving inherent optical properties from water color: a multiband quasi-analytical algorithm for optically deep waters. *Applied Optics*, **41**, pp. 5755-5772.

LENOBLE, J., HERMAN, M., DEUZÉ, J., LAFRANCE, B., SANTER, R., and TANRÉ, D., 2007, A successive order of scattering code for solving the vector equation of transfer in the earth's atmosphere with aerosols. *Journal of Quantitative Spectroscopy and Radiative Transfer*, **107**, pp. 479-507.

LINDELL, T., PIERSON, D., PREMAZZI, G., and ZILIOLI, E. (Eds.), 1999, *Manual for monitoring european lakes using remote sensing techniques*, pp. 164 (Luxembourg: Office for Official Publications of the European Communities).

MATTHEWS, M.W., 2010, Remote sensing of water quality parameters in Zeekoevlei, a hypertrophic, cyanobacteria-dominated lake, Cape Town, South Africa. M.Sc. thesis, University of Cape Town, Cape Town.

MAYO, M., GITELSON, A., YACOBI, Y.Z., and BEN-AVRAHAM, Z., 1995, Chlorophyll distribution in lake Kinneret determined from Landsat Thematic Mapper data. *International Journal of Remote Sensing*, **16**, pp. 175-182.

MENKEN, K.D., BREZONIK, P.L., and BAUER, M.E., 2006, Influence of chlorophyll and Colored Dissolved Organic Matter (CDOM) on lake reflectance spectra: implications for measuring lake properties by remote sensing. *Lake and Reservoir Management*, **22**, pp. 179-190.

MERTES, L.A.K., 2002, Remote sensing of riverine landscapes. *Freshwater Biology*, **47**, pp. 799-816.

METSAMAA, L., KUTSER, T., and STROEMBECK, N., 2006, Recognising cyanobacterial blooms based on their optical signature: a modelling study. *Boreal Environment Research*, **11**, pp. 493-506.

MIKSA, S., P. GEGE, and T. HEEGE, 2004, Investigations on the capability of CHRIS-Proba for monitoring of water constituents in Lake constance compared to MERIS. In *Proceedings of the 2nd CHRIS-PROBA workshop (SP-578)*, Frascati, Italy (Italy: ESA) pp. 38-30.

MILLER, R.L., and MCKEE, B.A., 2004, Using MODIS Terra 250 m imagery to map concentrations of total suspended matter in coastal waters. *Remote Sensing of Environment*, **93**, pp. 259-266.

MISHRA, S., MISHRA, D.R., and SCHLUCHTER, W.M., 2009, A Novel Algorithm for Predicting Phycocyanin Concentrations in Cyanobacteria: A Proximal Hyperspectral Remote Sensing Approach. *Remote Sensing*, **1**, pp. 758-775.

MITTENZWEY, K., GITELSON, A., ULLRICH, S., and KONDRATIEV, K., 1992, Determination of chlorophyll a of inland waters on the basis of spectral reflectance. *Limnology and Oceanography*, **37**, pp. 147-149.

MOBLEY, C., 1994, *Light and Water: radiative transfer in natural waters*, pp. 592 (San Diego: Academic Press).

MORAN, M.S., BRYANT, R., THOME, K., NOUVELLON, W.N.Y., GONZALES-DUGO, M.P., QI, J., and CLARKE, T.R., 2001, A refined empirical line approach for reflectance factor retrieval from Landsat-5 TM and Landsat-7 ETM. *Remote Sensing of Environment*, **78**, pp. 71-82.

MOREL, A., and PRIEUR, L., 1977, Analysis of variations in ocean color. *Limnology and Oceanography*, **22**, pp. 709-722.

MOSES, W., GITELSON, A., BERDNIKOV, S., and POVAZHNYY, V., 2009a, Satellite estimation of chlorophyll-a concentration using the red and NIR bands of MERIS—the Azov Sea case study. *IEEE Geoscience and Remote Sensing Letters*, **6**, pp. 845-849.

MOSES, W.J., GITELSON, A.A., BERDNIKOV, S., and POVAZHNYY, V., 2009b, Estimation of chlorophyll-a concentration in case II waters using MODIS and MERIS data—successes and challenges. *Environmental Research Letters*, **4**, pp. 045005.

NAS, B., KARABORK, H., EKERCIN, S., and BERKTAY, A., 2009, Mapping chlorophyll-a through in-situ measurements and Terra ASTER satellite data. *Environmental Monitoring and Assessment*, **157**, pp. 375-382.

NASA, 2008, Landsat 7 science data users handbook. Available online at: http://landsathandbook.gsfc.nasa.gov/handbook/handbook_toc.html (accessed 4 November 2008).

NAVALGUND, R.R., JAYARAMAN, V., and ROY, P.S., 2007, Remote sensing applications: an overview. *Current science*, **93**, pp. 1747-1766.

NECHAD, B., V. DE CAUWER, Y. PARK, and K. G. RUDDICK, 2003, Suspended Particulate Matter (SPM) mapping from MERIS imagery. Calibration of a regional algorithm for the Belgian coastal waters. In *Proceedings of the MERIS Users workshop*, Frascati, 10-13 November 2003 (Rome, Italy: ESA Special Publication SP-549) pp. 52.0.

NECHAD, B., RUDDICK, K.G., and PARK, Y., 2010, Calibration and validation of a generic multisensor algorithm for mapping of Total Suspended Matter in turbid waters. *Remote Sensing of Environment*, **114**, pp. 854-866.

NEUKERMANS, G., RUDDICK, K., BERNARD, E., RAMON, D., NECHAD, B., and DESCHAMPS, P.Y., 2009, Mapping total suspended matter from geostationary satellites: a feasibility study with SEVIRI in the Southern North Sea. *Optics Express,* **17**, pp. 14029-14052.

ODERMATT, D., HEEGE, T., NIEKE, J., KNEUBÜHLER, M., and ITTEN, K., 2008, Water quality monitoring for Lake Constance with a physically based algorithm for MERIS data. *Sensors,* **8**, pp. 4582-4599.

OLMANSON, L.G., BAUER, M.E., and BREZONIK, P.L., 2008, A 20-year Landsat water clarity census of Minnesota's 10,000 lakes. *Remote Sensing of Environment,* **112**, pp. 4086-4097.

ONDERKA, M., and PEKAROVA, P., 2008, Retrieval of suspended particulate matter concentrations in the Danube River from Landsat ETM data. *Science of the Total Environment,* **397**, pp. 238-243.

O'REILLY, J.E., MARITORENA, S., MITCHELL, B.G., SIEGEL, D.A., CARDER, K.L., GARVER, S.A., KAHRU, M., and MCCLAIN, C., 1998, Ocean color chlorophyll algorithms for SeaWiFS. *Journal of Geophysical Research,* **103**, pp. 24937-24953.

ORMECI, C., SERTEL, E., and SARIKAYA, O., 2009, Determination of chlorophyll-a amount in Golden Horn, Istanbul, Turkey using IKONOS and in situ data. *Environmental Monitoring and Assessment,* **155**, pp. 83-90.

ÖSTLUND, C., FLINK, P., STROMBECK, N., PIERSON, D., and LINDELL, T., 2001, Mapping of the water quality of Lake Erken, Sweden, from imaging spectrometry and Landsat Thematic Mapper. *The Science of the Total Environment,* **268**, pp. 139-154.

OYAMA, Y., MATSUSHITA, B., FUKUSHIMA, T., MATSUSHIGE, K., and IMAI, A., 2009, Application of spectral decomposition algorithm for mapping water quality in a turbid lake (Lake Kasumigaura, Japan) from Landsat TM data. *ISPRS Journal of Photogrammetry and Remote Sensing,* **64**, pp. 73-85.

OYAMA, Y., MATSUSHITA, B., FUKUSHIMA, T., NAGAI, T., and IMAI, A., 2007, A new algorithm for estimating chlorophyll-a concentration from multi-spectral satellite data in case II waters: a simulation based on a controlled laboratory experiment. *International Journal of Remote Sensing,* **28**, pp. 1437-1453.

PATTIARATCHI, C., LAVERY, P., WYLLLIE, A., and HICK, P., 1994, Estimates of water quality in coastal waters using multi-date Landsat Thematic Mapper data. *International Journal of Remote Sensing,* **15**, pp. 1571-1584.

PEÑA-MARTINEZ, R., J. A. DOMÍNGUEZ-GÓMEZ, C. DE HOYOS, and A. RUIZ-VERDÚ, 2004, Mapping of photosynthetic pigments in Spanish reservoirs. In *Proceedings of MERIS User Workshop (ESA SP-549), 10-13 November 2003,* Frascati, Italy (Published on CDROM: ESA-ESRIN) pp. 16.1.

PETUS, C., CHUST, G., GOHIN, F., DOXARAN, D., FROIDEFOND, J.M., and SAGARMINAGA, Y., 2009, Estimating turbidity and total suspended matter in the Adour River plume (South Bay of Biscay) using MODIS 250-m imagery. *Continental Shelf Research,*

POWER, M.E., BROZOVIC, N., BODE, C., and ZILBERMAN, D., 2005, Spatially explicit tools for understanding and sustaining inland water ecosystems. *Frontiers in Ecology and the Environment,* **3**, pp. 47-55.

PREISENDORFER, R.W., 1986, Secchi disk science: Visual optics of natural waters. *Limnology and Oceanography,* **31**, pp. 909-926.

PREISENDORFER, R. W., 1976, *Hydrologic Optics*, pp. 1757 (Honolulu: U.S. Dept of Commerce, NOAA, ERL, Pacific Marine Environmental Laboratory).

RAHMAN, H., and DEDIEU, G., 1994, SMAC: a simplified method for the atmospheric correction of satellite measurements in the solar spectrum. *International Journal of Remote Sensing*, **15**, pp. 123-143.

RANDOLPH, K., WILSON, J., TEDESCO, L., LI, L., PASCUAL, D.L., and SOYEUX, E., 2008, Hyperspectral remote sensing of cyanobacteria in turbid productive water using optically active pigments, chlorophyll a and phycocyanin. *Remote Sensing of Environment*, **112**, pp. 4009-4019.

REES, G., 2001, *Physical principles of remote sensing*, pp. 372 (Cambridge: Cambridge University Press).

REINART, A., and KUTSER, T., 2006, Comparison of different satellite sensors in detecting cyanobacterial bloom events in the Baltic Sea. *Remote Sensing of Environment*, **102**, pp. 74-85.

RICHARDSON, L.L., 1996, Remote Sensing of Algal Bloom Dynamics. *Bioscience*, **46**, pp. 492-501.

RITCHIE, J.C., ZIMBA, P.V., and EVERITT, J.H., 2003, Remote sensing techniques to assess water quality. *Photogrammetric Engineering and Remote Sensing*, **69**, pp. 695-704.

RUDDICK, K.G., DE CAUWER, V., PARK, Y.J., and MOORE, G., 2006, Seaborne measurements of near infrared water-leaving reflectance: The similarity spectrum for turbid waters. *Limnology and Oceanography*, **51**, pp. 1167-1179.

RUIZ-VERDÚ, A., J. A. DOMÍNGUEZ-GÓMEZ, and R. PEÑA-MARTÍNEZ, 2005, Use of CHRIS for monitoring water quality in Rosarito reservoir. In *Proceedings of the Third CHRIS/Proba Workshop, 21-23 March, ESRIN, Frascati, Italy*, (Paris: ESA) pp. SP-593.

RUIZ-VERDÚ, A., SIMIS, S.G.H., DE HOYOS, C., GONS, H.J., and PEÑA-MARTÍNEZ, R., 2008, An evaluation of algorithms for the remote sensing of cyanobacterial biomass. *Remote Sensing of Environment*, **112**, pp. 3996-4008.

SALAMA, M.S., and SHEN, F., 2010, Simultaneous atmospheric correction and quantification of suspended particulate matters from orbital and geostationary earth observation sensors. *Estuarine, Coastal and Shelf Science*, **86**, pp. 499-511.

SCHALLES, J.F., GITELSON, A.A., YACOBI, Y.Z., and KROENKE, A.E., 1998, Estimation of chlorophyll a from time series measurements of high spectral resolution reflectance in an eutrophic lake. *Journal of Phycology*, **34**, pp. 383-390.

SCHALLES, J.F., and YACOBI, Y.Z., 2000, Remote detection and seasonal patterns of phycocyanin, carotenoid and chlorophyll pigments in eutrophic waters. *Archiv fuer Hydrobiologie-Special Issues Advancements in Limnology*, **55**, pp. 153-168.

SCHILLER, H., and DOERFFER, R., 2005, Improved determination of coastal water constituent concentrations from MERIS data. *IEEE Transactions on Geoscience and Remote Sensing*, **43**, pp. 1585-1591.

SCHILLER, H., and DOERFFER, R., 1999, Neural network for emulation of an inverse model operational derivation of Case II water properties from MERIS data. *International Journal of Remote Sensing*, **20**, pp. 1735-1746.

SIMIS, S.G.H., PETERS, S.W.M., and GONS, H.J., 2005, Remote sensing of the cyanobacterial pigment phycocyanin in turbid inland water. *Limnology and Oceanography*, **50**, pp. 237-245.

SIMIS, S.G.H., RUIZ-VERDU, A., DOMINGUEZ-GOMEZ, J.A., PENA-MARTINEZ, R., PETERS, S.W.M., and GONS, H.J., 2007, Influence of phytoplankton pigment composition on remote sensing of cyanobacterial biomass. *Remote Sensing of Environment*, **106**, pp. 414-427.

STRAMSKI, D., BOSS, E., BOGUCKI, D., and VOSS, K.J., 2004, The role of seawater constituents in light backscattering in the ocean. *Progress in Oceanography*, **61**, pp. 27-56.

STRÖMBECK, N., G. CANDIANI, C. GIARDINO, and E. ZILIOLI, 2004, Water quality monitoring of Lake Garda using multi-temporal MERIS data. In *Proceedings of MERIS User Workshop (ESA SP-549) 10-13 November 2003, Frascati, Italy*, (Published on CDROM: ESA-ESRIN) pp. 17.1.

SUDHEER, K.P., CHAUBEY, I., and GARG, V., 2006, Lake water quality assessment from Landsat thematic mapper data using neural network: An approach to optimal band combination selection. *Journal of the American Water Resources Association*, **42**, pp. 1683-1695.

SVÁB, E., TYLER, A.N., PRESTON, T., PRÉSING, M., and BALOGH, K.V., 2005, Characterizing the spectral reflectance of algae in lake waters with high suspended sediment concentrations. *International Journal of Remote Sensing*, **26**, pp. 919-928.

THIEMANN, S., and KAUFMANN, H., 2000, Determination of chlorophyll content and trophic state of lakes using field spectrometer and IRS-1C satellite data in the Mecklenburg lake district, Germany. *Remote Sensing of Environment*, **73**, pp. 227-235.

TYLER, A.N., SVAB, E., PRESTON, T., PRÉSING, M., and KOVÁCS, W.A., 2006, Remote sensing of the water quality of shallow lakes: A mixture modelling approach to quantifying phytoplankton in water characterized by high-suspended sediment. *International Journal of Remote Sensing*, **27**, pp. 1521-1537.

VALLELY, L.A., 2008, Confounding constituents in remote sensing of phycocyanin. M.Sc. thesis, Department of Geography, Indiana University, Indiana.

VERMOTE, E.F., TANRE, D., DEUZE, J.L., HERMAN, M., and MORCETTE, J.J., 1997, Second Simulation of the Satellite Signal in the Solar Spectrum, 6S: an overview. *Geoscience and Remote Sensing, IEEE Transactions on*, **35**, pp. 675-686.

VINCENT, R.K., QIN, X.M., MCKAY, R.M.L., MINER, J., CZAJKOWSKI, K., SAVINO, J., and BRIDGEMAN, T., 2004, Phycocyanin detection from LANDSAT TM data for mapping cyanobacterial blooms in Lake Erie. *Remote Sensing of Environment*, **89**, pp. 381-392.

VOS, R.J., HAKVOORT, J.H.M., JORDANS, R.W.J., and IBELINGS, B.W., 2003, Multiplatform optical monitoring of eutrophication in temporally and spatially variable lakes. *The Science of the Total Environment*, **312**, pp. 221-243.

WANG, F., HAN, L., KUNG, H.T., and VAN ARSDALE, R.B., 2006, Applications of Landsat-5 TM imagery in assessing and mapping water quality in Reelfoot Lake, Tennessee. *International Journal of Remote Sensing*, **27**, pp. 5269-5283.

WANG, X.J., and MA, T., 2001, Application of remote sensing techniques in monitoring and assessing the water quality of Taihu Lake. *Bulletin of environmental contamination and toxicology*, **67**, pp. 863-870.

WANG, Y., XIA, H., FU, J., and SHENG, G., 2004, Water quality change in reservoirs of Shenzhen, China: detection using LANDSAT/TM data. *The Science of the Total Environment*, **328**, pp. 195-206.

WU, G.G., DE LEEUW, J., SKIDMORE, A.K., PRINS, H.H.T., and LIU, Y., 2008, Comparison of MODIS and Landsat TM5 images for mapping tempo-spatial dynamics of Secchi disk depths in Poyang Lake national nature reserve, China. *International Journal of Remote Sensing,* **29**, pp. 2183-2198.

WU, M., ZHANG, W., WANG, X., and LUO, D., 2009, Application of MODIS satellite data in monitoring water quality parameters of Chaohu Lake in China. *Environmental monitoring and assessment,* **148**, pp. 255-264.

YACOBI, Y.Z., GITELSON, A., and MAYO, M., 1995, Remote sensing of chlorophyll in Lake Kinneret using high spectral-resolution radiometer and Landsat TM: spectral features of reflectance and algorithm development. *Journal of Plankton Research,* **17**, pp. 2155-2173.

YANG, D., and PAN, D., 2006, Hyperspectral retrieval model of phycocyanin in case II waters. *Chinese Science Bulletin,* **51**, pp. 149-153.

ZANEVELD, J.R.V., 1995, A theoretical derivation of the dependence of the remotely sensed reflectance of the ocean on the inherent optical properties. *Journal of Geophysical Research-Part C-Oceans-Printed Edition,* **100**, pp. 13.135-13.142.

ZHANG, Y., PULLIAINEN, J., KOPONEN, S., and HALLIKAINEN, M., 2002, Application of an empirical neural network to surface water quality estimation in the Gulf of Finland using combined optical data and microwave data. *Remote Sensing of Environment,* **81**, pp. 327-336.

ZIMBA, P.V., and GITELSON, A., 2006, Remote estimation of chlorophyll concentration in hyper-eutrophic aquatic systems: Model tuning and accuracy optimization. *Aquaculture,* **256**, pp. 272-286.

Table 1.
Recent remote sensing studies in inland and near-coastal waters using empirical techniques (see Appendix A for a description of acronyms and abbreviations).

| Year | *Country* | *Study area* | *Data type*† | *Atmos. corr.* | *WQPs*‡ | *Data range*§ | *Statistical technique* | *Bands/algorithm*¶ | $r^2$ | *RMSE* \| *(%)* | *N* | *Reference* |
|---|---|---|---|---|---|---|---|---|---|---|---|---|
| ***Studies using multi-spectral ocean colour sensors (including simulations)*** | | | | | | | | | | | | |
| 2010 | France | Bay of Biscay | Sl. MODIS (250m) | MODIS Level 2G | TSS | 0.3–145.6 | Poly($2^{nd}$) | B2 | 0.96 | 61 | 74 | (Petus *et al.* 2009) |
| | | | | | Turb | 0.01 – 188.2 | Poly($2^{nd}$) | B2 | 0.95 | 378 | 74 | |
| 2009 | Malawi | Lake Malawi | MODIS | MODIS Level 2G | Chl *a* | 0.1 – 0.4 | LR | *R*443/*R*551 | 0.58 | - | 5 | (Chavula *et al.* 2009) |
| 2009 | France | Gironde Estuary | MODIS AQUA (250m) | MODIS Level 2G | TSS | 77–2182 | LR | B2/B1 | 0.82 | 245 | 75 | (Doxaran *et al.* 2009) |
| 2009 | US | Fremont State Lakes | Sl. MERIS | NA | Chl *a* | ~ 2–50 | NLR | $[R670^{-1}–R710^{-1}]\times R750$ | 0.93 | 5.1 $mg.m^{-3}$ | 77 | (Gitelson *et al.* 2009) |
| 2009 | Russia | Taganrog Bay, Azov Sea | MERIS | MERIS Level 2 | Chl *a* | 0.63 – 65.51 | LR | *R*708/*R*665 | 0.97 | 3.65 $mg.m^{-3}$ | 18 | (Moses *et al.* 2009a) |
| | | | MERIS | MERIS Level 2 | Chl *a* | 0.63 – 65.51 | LR | $[R665^{-1}–R708^{-1}]\times R753$ | 0.95 | 5.02 $mg.m^{-3}$ | 18 | |
| 2009 | Russia | Azov Sea | MERIS | MERIS Level 2 | Chl *a* | | LR | $[R665^{-1}–R708^{-1}]\times R753$ | 0.93 | - | 7 | (Moses *et al.* 2009b) |
| | | Dnieper Estuary | MODIS | MUMM | Chl *a* | | LR | *R*748/*R*667 | 0.6 | - | 7 | |
| 2009 | China | Chaohu Lake | MODIS | 6S | Chl *a* | 5.2 – 33.9 | MLR | LnB2+LnB9–Ln(B3–B2)/B2 | 0.63 | - | 40 | (Wu *et al.* 2009) |
| | | | | | $z_{SD}$ | 0.25 – 1.2 | MLR | LnB4/B10+(B1+B2)/B3+B4 | 0.63 | - | 40 | |
| 2008 | Baltic Sea | Himmerfjärden Bay | Sl. MERIS | NA | $z_{SD}$ | ~3–6 | TL-LR | *R*490/*R*620 | 0.79 | - | 23 | (Kratzer *et al.* 2008) |
| 2008 | Germany | Lake Constance | MERIS | MIP | Chl *a* | 0–20 | Analytical | MIP | 0.79 | - | 8 | (Odermatt *et al.* 2008) |
| | | | | | TSS | 0–10 | Analytical | MIP | - | - | - | |
| | | | | | $a_{CDOM}$ | 0–0.3 | Analytical | MIP | - | - | - | |
| 2008 | China | Poyang Lake | MODIS | MODIS Level 2G | $z_{SD}$ | 0.06–2.84 | LT-MLR | B3, B1 | 0.88 | 37 | 71 | (Wu *et al.* 2008) |
| | | | LS TM | COST | $z_{SD}$ | 0.32–2.16 | LT-MLR | TM1, TM3 | 0.83 | 20 | 25 | |
| 2007 | US | Tampa Bay | MODIS | RTC | Turb | 0.9–8.0 | LR | B1 | 0.73 | - | 43 | (Chen *et al.* 2007) |
| 2007 | Netherlands; Spain | 59 Lakes | Sl. MERIS | NA | PC | ~ 0–1100 | SA | *R*709/*R*620 | 0.90 | - | 223 | (Simis *et al.* 2007) |
| 2006 | Gulf of Finland | Baltic Sea | MERIS | None | Chl *a* | 22–95 | LR | *L*709/*L*665 | 0.87 | 22 | 51 | (Koponen *et al.* 2007) |
| | | | | | TSS | 2.9–12 | LR | *L*709/(*L*560+*L*665) | 0.92 | 16 | 51 | |
| | | | | | $a_{CDOM}$ | 1.29–2.15 | LR | *L*665/*L*490 | 0.96 | 5 | 51 | |
| 2005 | Italy | Lake Guarda | MERIS | 6S, DDV | Chl *a* | ~ 2–11 | LR | *L*560/*L*665 | 0.49 | 1.20 $mg.m^{-3}$ | 7 | (Candiani *et al.* 2005) |
| 2005 | Italy | Lake Guarda | Sl. MIVIS MERIS | NA | Chl *a* | 3.5–8.9 | LR | (*L*440–*L*780)/(*L*480–*L*700) | 0.69 | 9 | 22 | (Giardino *et al.* 2005) |

| Year | *Country* | *Study area* | *Data type*† | *Atmos. corr.* | *WQPs*‡ | *Data range*§ | *Statistical technique* | *Bands/algorithm*¶ | $r^2$ | *RMSE* \| *(%)* | *N* | *Reference* |
|---|---|---|---|---|---|---|---|---|---|---|---|---|
| | | | MERIS | None | Chl *a* | 0.2–2.5 | LR | *L*489 | 0.83 | 26 | 31 | |
| 2005 | Netherlands | 2 lakes | Sl. MERIS | NA | PC | 0.8–79.8 | SA | *R*720/*R*620 | 0.94 | 19.7 | 33 | (Simis *et al.* 2005) |
| 2004 | Austria; Italy | 4 Austrian Lakes; Lake Guarda | MERIS | 6S | Chl *a* | 1.0–5.6 | LR | *L*665/*L*560 | 0.75 | 0.66 $mg.m^{-3}$ | 29 | (Floricioiu *et al.* 2004) |
| 2004 | Finland | Finnish Lakes | MODIS | None | Classes | 1–4 | Classification | B1 | 0.8* | 19.8%* | 20391 | (Koponen *et al.* 2004) |
| 2004 | US | Gulf of Mexico | MODIS | DOS | TSS | ~ 1–55 | LR | B1 | 0.89 | 2.18 $mg.l^{-1}$ | 52 | (Miller and McKee 2004) |
| 2004 | Italy | Lake Garda | MERIS | ELM | Chl *a* | 0.7-2.5 | Poly($2^{nd}$) | *L*620/*L*709 | 0.76 | 0.27 $mg.m^{-3}$ | 12 | (Strömbeck *et al.* 2004) |
| 2003 | US | Gulf of Mexico | Sl. SeaWiFS | NA | $a_{CDOM}$ | 0.4–0.01 | LT-LR | *R*443/*R*510 | 0.86 | - | 19 | (D'Sa and Miller 2003) |
| 2003 | Austria | 3 Austrian Lakes | Sl. ROSIS MERIS | 6S | Chl *a* | 1.42–5.17 | LR | *L*620/*L*490 + *L*560/*L*510 | 0.93 | 1.0 $mg.m^{-3}$ | 13 | (Floricioiu *et al.* 2003) |
| 2003 | Finland | Lake Hiidenvesi | Sl. MERIS (AISA) | NA | Chl *a* | 6–44 | LR | *L*705/*L*662 | 0.98 | 11.1 | 12 | (Kallio *et al.* 2003) |
| 2003 | Netherlands | Lakes IJssel and Marken | SeaWiFS | SeaDAS | Chl *a* | ~ 5–160 | Analytical | 2 step SeaWiFS | - | 27 | 14 | (Vos *et al.* 2003) |
| | | | | | TSS | ~ 10–250 | Analytical | 3 step SeaWiFS | - | 38 | 14 | |
| 2002 | Sweden | Lake Märalen | Sl. CASI MERIS | 6S | Chl *a* | 2.5–18.9 | SA | *R*705/*R*664 | 0.88 | - | 570 | (Ammenberg *et al.* 2002) |
| | | | | | SPIM | 0.5–2.3 | SA | *R*705/*R*664 | 0.83 | 0.34 $mg.m^{-3}$ | 570 | |
| | | | | | $a_{CDOM}$ | 1.13–2.07 | SA | *R*664/*R*550 | - | - | 2 | |
| 2002 | Netherlands | Ijssel Lagoon | Sl. Spec. MERIS | NA | Chl *a* | 3–185 | LR | *L*708/*L*664 | 0.96 | 8.3 $mg.m^{-3}$ | 114 | (Gons *et al.* 2002, 2005) |
| 2002 | Finland | Finnish Lakes | Sl. MERIS (AISA) | None | Chl *a* | 1.3–100 | LR | (*L*700–*L*781)/(*L*662–*L*781) | 0.94 | - | 80 | (Koponen *et al.* 2002) |
| | | | | | $z_{SD}$ | 0.4–7.0 | LR | (*L*521–*L*781)/(*L*700–*L*781) | 0.93 | - | 102 | |
| | | | | | Turb | 0.4–26 FNU | LR | *L*714 | 0.85 | - | 99 | |
| 2001 | Sweden | Lakes Erken and Märalen | Sl. CASI MERIS | 6S | Chl *a* | 2.9–50.6 | LR | *R*550 | 0.94 | - | 13 | (Flink *et al.* 2001) |
| | | | | | Chl *a* | 2.9–50.7 | LR | *R*708/*R*678 | 0.84 | - | 13 | |
| | | | | | Chl *a* | 2.9–50.8 | MLR | *R*708/*R*678 + *R*643/*R*628 | 0.87 | - | 13 | |
| | | | | | Chl *a* | 2.9–50.9 | PCA; MLR | PC1 + PC2 + PC3 + PC4 | 0.96 | - | 13 | |
| 2001 | Finland | Lakes | Sl. MERIS (AISA) | None | Chl *a* | 1.3–100 | LR | (*L*705–*L*754)/(*L*665–*L*754) | 0.9 | 37 | 85 | (Härmä *et al.* 2001) |
| | | | | | TSS | 0.7–23 | LR | *L*705–*L*754 | 0.81 | 34 | 67 | |
| | | | | | $z_{SD}$ | 0.4–7.0 | LR | (*L*490–*L*754)/(*L*620–*L*754) | 0.83 | 35 | 85 | |
| 2001 | Finland | 11 Lakes | Sl. MERIS (AISA) | MODTRAN | Chl *a* | 1–100 | LR | *L*702/*L*674 | 0.91 | 29 | 88 | (Kallio *et al.* 2001) |

| Year | Country | Study area | Data type† | Atmos. corr. | WQPs‡ | Data range§ | Statistical technique | Bands/algorithm¶ | $r^2$ | RMSE \| (%) | N | Reference |
|---|---|---|---|---|---|---|---|---|---|---|---|---|
| | | | | | TSS | 0.7–32 | LR | *R*710 | 0.85 | 32 | 74 | |
| | | | | | $z_{SD}$ | 0.4–7 | LR | (*L*492–*L*751)/(*L*622–*L*751) | 0.86 | 30 | 103 | |
| | | | | | $a_{CDOM}$ | 1.2–14 | LR | (*L*571–*L*607)/*L*607 | 0.84 | 20 | 47 | |
| | | | | | Turb | 0.4–26 FNU | LR | *R*710 | 0.93 | 23 | 105 | |
| ***Studies using multi-spectral high spatial resolution sensors*** | | | | | | | | | | | | |
| 2009 | China | Lake Chagan, Xinmiao, Kuli | LS TM | 6S | $z_{SD}$ | 0.22 – 0.79 | LT-LR | TM3/TM2 | 0.91 | 0.03 m | 15 | (Duan *et al.* 2009) |
| 2009 | Turkey | Lake Beysehir | ASTER | None | Chl *a* | 0.37 – 4.11 | MLR | B1, B2, B3, B4 | 0.86 | - | 23 | (Nas *et al.* 2009) |
| 2009 | Turkey | Golden Horn inlet | IKONOS | Erdas ATCOR 2 | Chl *a* | ~ 0.1 – 2.14 | MLR | B1, B2, B3, B4 | 0.88 | - | 9 | (Ormeci *et al.* 2009) |
| 2009 | Japan | Lake Kasumigaura | Sl. LS | NA | Chl *a* | 0–127 | SDA | TM1, TM2, TM3 | 0.87 | 16.2 $mg.m^{-3}$ | 55 | (Oyama *et al.* 2009) |
| 2008 | Taiwan | Feitsui Reservoir | LS 7 ETM+ | None | Chl *a* | 0.48–4.02 | MLR | ETM1, ETM2, ETM3, ETM4, ETM5, ETM7 | 0.68 | 0.37 $mg.m^{-3}$ | 24 | (Chen *et al.* 2008) |
| | | | | | Chl *a* | 0.48–4.03 | GEGA | ETM1, ETM4, ETM5, ETM7 | 0.79 | 0.30 $mg.m^{-3}$ | 24 | |
| 2008 | Finland | Southern Lakes | LS ETM+ | SMAC | $z_{SD}$ | 0.5–5.5 | LR | TM1/TM3 | 0.78 | 26.9 | 131 | (Kallio *et al.* 2008) |
| | | | | | $a_{CDOM}$ | 1.0–12.2 | NLR | TM2/TM3 | 0.83 | 22.3 | 29 | |
| | | | | | Turb | 0.6–15 FNU | LR | TM3 | 0.86 | 28.7 | 80 | |
| 2008 | US | Minnesota's lakes | LS TM, ETM+ | None | $z_{SD}$ | 0.15–14.6 | LT-MLR | TM1/TM3, TM1 | 0.71 – 0.96 | 14.1 – 40.6 | 13 - 278 | (Olmanson *et al.* 2008) |
| 2008 | Slovakia | Danube River | LS 7 ETM+ | None | TSS | 19.5–57.5 | LR | ETM4 | 0.93 | 1.79 $mg.l^{-1}$ | 10 | (Onderka and Pekarova 2008) |
| 2007 | Turkey | Ömerli Dam | LS 7 ETM+ | DOS | Chl *a* | 1.2–2.5 | MLR | ETM1, ETM2, ETM3, ETM4 | 0.58 | 49 | 6 | (Alparslan *et al.* 2007) |
| | | | | | TSS | 0.4–2.9 | MLR | ETM1, ETM2, ETM3, ETM5 | 0.99 | 1 | 6 | |
| | | | | | $z_{SD}$ | 2.5–3.4 | MLR | ETM1, ETM2, ETM3, ETM6 | 0.99 | 2 | 6 | |
| 2007 | China | Lake Chagan | LS TM | None | Chl *a* | 6.3–58.2 | LR | TM4/TM3 | 0.67 | 2.06 $mg.m^{-3}$ | 20 | (Duan *et al.* 2007) |
| | | | Spec. | NA | Chl *a* | 6.3–58.2 | LT-LR | Ln(*R*700/*R*670) | 0.75 | - | 54 | |
| 2007 | US | Charles River | IKONOS | None | Turb | 1.9–7.3 | LR | $DN_{632-698}$ | 0.7 | - | 3084 | (Hellweger *et al.* 2007) |
| 2006 | France | Gironde Estuary | Sl. SPOT | 6S, DOS | TSS | 10–2000 | NLR | XS3/XS1 | 0.89 | - | 132 | (Doxaran *et al.* 2006) |
| | | | Sl. LS ETM+ | 6S, DOS | TSS | 10–2000 | NLR | ETM4/ETM2 | 0.88 | - | 132 | |
| 2006 | US | Beaver Reservoir | LS TM | None | Chl *a* | ~ 1.7–10 | ANN; LR | TM1, TM2 | 0.54 | 12.34 $mg.m^{-3}$ | ~25 | (Sudheer *et al.* 2006) |
| | | | | | TSS | ~ 0–11.5 | ANN; LR | TM1, TM2, TM3, TM4 | 0.98 | 2.02 $mg.m^{-3}$ | ~25 | |

| Year | *Country* | *Study area* | *Data type*† | *Atmos. corr.* | *WQPs*‡ | *Data range*§ | *Statistical technique* | *Bands/algorithm*¶ | $r^2$ | *RMSE* \| *(%)* | *N* | *Reference* |
|---|---|---|---|---|---|---|---|---|---|---|---|---|
| 2006 | Central Europe | Lake Balaton | LS TM; ETM+ | DOS | Chl *a* | ~ 5–115 | LMM | TM1, TM2, TM3 OR ETM1, ETM2, ETM3 | 0.95 | - | 11 | (Tyler *et al.* 2006) |
| | | | | | TSS | ~ 5–50 | LR | TM3 | 0.89 | - | 11 | |
| 2006 | US | Reelfoot Lake | LS 5 TM | Radiometric | Chl *a* | 66–189 | MLR | TM2, TM3 | 0.71 | - | 18 | (Wang *et al.* 2006) |
| | | | | | TSS | 11.5–33.5 | MLR | TM2, TM3, TM4 | 0.52 | - | 18 | |
| | | | | | $z_{SD}$ | 16–33 | MLR | TM2, TM3 | 0.59 | - | 18 | |
| | | | | | Turb | 20.0–4.1 | MLR | TM2, TM3 | 0.54 | - | 18 | |
| 2005 | US | 15 Minnesota Lakes | LS TM | None | Chl *a* | 2.1–279 | LT-MLR | TM1, TM1/TM3 | 0.88 | - | 15 | (Brezonik *et al.* 2005) |
| | | | | | Turb | 0.3–155 | LT-MLR | TM3 | 0.84 | - | 15 | |
| | | | | | $z_{SD}$ | 0.15–4.4 | LT-MLR | TM1, TM1/TM3 | 0.91 | - | 39 | |
| | | | | | $a_{CDOM}$ | 0.6–19.4 | LT-MLR | TM1, TM1/TM4 | 0.77 | - | 15 | |
| 2005 | US | Pensacola Bay | LS 7 ETM+ | Radiometric | Chl *a* | 1.1–23.2 | LT-LR | Log ETM1/log ETM3 | 0.67 | 19 | 16 | (Han and Jordan 2005) |
| 2005 | Finland; Sweden | Many Lakes | ALI | ELM | $a_{CDOM}$ | 0.68–11.13 | NLR | $L_{525\text{-}605}/L_{630\text{-}690}$ | 0.73 | - | 30 | (Kutser *et al.* 2005) |
| 2005 | Central Europe | Lake Balaton | Sl. LS | NA | TSS | 2–40.5 | LR | TM2/TM3 | 0.88 | - | 10 | (Sváb *et al.* 2005) |
| 2004 | Taiwan | Techi Reservoir | LS TM | DOS | Cell density | ~ 50–2400 | LT-MLSR | TM1, TM2, TM3, TM4 | 0.73 | - | 120 | (Chang *et al.* 2004) |
| 2004 | US | New York Harbour | LS TM | Radiometric | $z_{SD}$ | ~ 0.45–2 | LT-LR | Log TM3 | 0.85 | - | 21 | (Hellweger *et al.* 2004) |
| | | | | | Chl *a* | ~ 5–50 | LT-LR | Log(TM2/TM3) | 0.78 | - | 16 | |
| 2004 | US | Lake Erie | LS 5 TM | DOS | PC | ~ 7.5–19 | MLR | TM1, TM2, TM3, TM4; TM5 | 0.63 | - | 20 | (Vincent *et al.* 2004) |
| | | | LS 7 ETM+ | DOS | PC | ~ 0.9–4.9 | MLR | ETM1, ETM2, ETM3, ETM4, ETM5 | 0.78 | 15 | 30 | |
| | | | | | Turb | ~ 14.2–1.3 | MLR | ETM3/ETM2 | 0.85 | 9 | 30 | |
| 2002 | France | Gironde, Loire Estuaries | Sl. SPOT | NA | TSS | 15–2500 | NLR | XS3/XS1 | 0.93 | - | 200 | (Doxaran *et al.* 2003) |
| | | | Sl. LS | NA | TSS | 15–2500 | NLR | TM4/TM2 | 0.88 | - | 200 | |
| | | | Sl. SeaWiFS | NA | TSS | 15–2500 | NLR | *R*865/*R*555 | 0.90 | - | 200 | |
| 2002 | France | Gironde Estuary | Sl. SPOT | 6S | TSS | 35–2072 | LR | XS3/XS1 | 0.93 | < 38 | 42 | (Doxaran *et al.* 2002) |
| 2002 | Netherlands | Southern Frisian Lakes | SPOT HRV; LS 5 TM | MODTRAN-3 | TSS | 3–411 | Analytical | (TM2 + TM3)/2 OR (XS1 + XS2)/2 | 0.99 | - | - | (Dekker *et al.* 2002) |
| 2002 | US | Minnesota Lakes | LS TM | ELM | $z_{SD}$ | ~0.5–5 | LT-MLR | TM1/TM3, TM1 | 0.71 – 0.92 | ~28 | 20 – 50 | (Kloiber *et al.* 2002) |
| 2002 | Finland | Gulf of Finland | LS TM SAR | None | Chl *a* | 2.0–7.7 | NN | TM1, ..., TM7, SAR | 0.92 | 11.2 | 53 | (Zhang *et al.* 2002) |

| Year | *Country* | *Study area* | *Data type*† | *Atmos. corr.* | *WQPs*‡ | *Data range*§ | *Statistical technique* | *Bands/algorithm*¶ | $r^2$ | *RMSE* \| *(%)* | *N* | *Reference* |
|---|---|---|---|---|---|---|---|---|---|---|---|---|
| | | | | | TSS | 1.6–11.0 | NN | TM1, ..., TM7, SAR | 0.91 | 15.2 | 53 | |
| | | | | | $z_{SD}$ | 0.67–4.2 | NN | TM1, ..., TM7, SAR | 0.95 | 7.3 | 53 | |
| | | | | | Turb | 1.0–7.5 FNU | NN | TM1, ..., TM7, SAR | 0.96 | 11.2 | 53 | |
| 2001 | Italy | Lake Guarda | LS TM | RTC - DOS | Chl *a* | 3.0–6.0 | LR | (TM1–TM3)/TM2 | 0.82 | 37 | 5 | (Brivio *et al.* 2001) |
| | | | | | Chl *a* | 1.9–3.2 | LT-MLR | Ln TM1–Ln TM2 | 0.68 | 49 | 5 | |
| 2001 | Italy | Lake Iseo | LS TM | DOS | Chl *a* | 5.5–7.7 | MLR | TM1, TM2 | 0.99 | 5.4 | 4 | (Giardino *et al.* 2001) |
| | | | | | $z_{SD}$ | 4.6–6.8 | LR | TM1/TM2 | 0.85 | 45 | 4 | |
| 2001 | Southern Finland | Lakes | Sl. LS (AISA) | NA | TSS | 0.7–23 | LT-LR | (TM1–TM4)/ (TM3–TM4) | 0.73 | 52 | 67 | (Härmä *et al.* 2001) |
| | | | | | Turb | - | LT-LR | (TM1–TM4)/ (TM3–TM4) | 0.88 | 44 | 83 | |
| | | | | | $z_{SD}$ | 0.4–7.0 | LR | (TM1–TM4)/ (TM3–TM4) | 0.81 | 34 | 85 | |
| 2001 | Sweden | Lake Erken | LS TM | 6S | Chl *a* | 2.1–27.4 | CHROM | TM1/TM1+TM2+TM3 | 0.93 | - | 19 | (Östlund *et al.* 2001) |
| | | | | | Chl *a* | 2.1–27.4 | LT-LR | Log(TM1/TM2) | 0.88 | - | 19 | |
| | | | | | TSS | 1.45–5.25 | LR | TM1 | 0.95 | - | 19 | |
| 2001 | China | Lake Taihu | LS TM | None | TSS | 10–107 | LT-MLR | Ln(TM3 + TM4)/ (TM1 + TM2) | - | - | 15 | (Wang and Ma 2001) |
| | | | | | $z_{SD}$ | 0.2–0.5 | PCA | LnTM1, LnTM2, LnTM3, LnTM5, LnTM7 | - | - | 15 | |
| 2000 | Germany | Mecklenburg Lake District | LISS-III | MODTRAN | Chl *a* | ~ 2 –63 | LSU | LISS1, LISS2, LISS3 | 0.85 | 3.6 $mg.m^{-3}$ | 11 | (Thiemann and Kaufmann 2000) |
| 1996 | Israel | 4 wastewater reservoirs | SPOT | LOWTRAN 7 | Chl *a* | 1.3–1600 | BOM;PCA | XS1, XS2, XS3 | - | - | 4 | (Dor and Ben-Yosef 1996) |
| | | | | | TSS | 2–195 | BOM;PCA | XS1, XS2, XS3 | - | - | 4 | |
| 1996 | Israel | Haifa Bay | Sl. LS | NA | Chl *a* | 2–70 | LT-LR | Log(TM3/TM1) | 0.74 | - | 18 | (Gitelson *et al.* 1996) |
| 1995 | Israel | Lake Kinneret | Sl. LS | Fraser *et al.* 1992 | Chl *a* | 3.1 – 7.3 | NLR | (TM1–TM3)/TM2 | 0.71 | 0.68 $mg.m^{-3}$ | 20 | (Mayo *et al.* 1995) |
| 1995 | Israel | Lake Kinneret | Spec. | NA | Chl *a* | 5.1–185 | LR | *R*max./*R*670 | 0.95 | 3.4 | 41 | (Yacobi *et al.* 1995) |
| | | | | | Chl *a* | 5.1–186 | LR | $RLH_{660\text{-}850}$ | 0.96 | 3.2 | 41 | |
| | | | LS TM | RTC | Chl *a* | 5.1–187 | LR | TM4/TM3 | 0.79 | 4 | 40 | |
| 1989 | US | Lake Michigan | SPOT HRV | Radiometric | $z_{SD}$ | 0.6–2.0 | LT-LR | XS3 | 0.83 | 20 | 11 | (Lathrop and Lillesand 1989) |
| | | | | | Turb | 11.9–1.2 | LT-LR | (XS2/XS1) + XS3 | 0.88 | 29 | 11 | |
| | | | | | TSS | 4.6–28.9 | LT-LR | (XS2/XS1) + XS3 | 0.93 | 19 | 11 | |
| 1986 | US | Lake Michigan | LS TM | None | Chl *a* | 1.0–50.3 | LT-LR | Ln TM2 | 0.98 | 1.04 $mg.m^{-3}$ | 13 | (Lathrop and Lillesand 1986) |
| | | | | | $z_{SD}$ | 0.5–9 | LT-LR | Ln TM2 | 0.98 | 1.05 m | 9 | |

| Year | *Country* | *Study area* | *Data type*† | *Atmos. corr.* | *WQPs*‡ | *Data range*§ | *Statistical technique* | *Bands/algorithm*¶ | $r^2$ | *RMSE* \| *(%)* | *N* | *Reference* |
|---|---|---|---|---|---|---|---|---|---|---|---|---|
| | | | | | Turb | 12–0.54 | LT-LR | Ln TM3 | 0.99 | 1.04 | 13 | |
| ***Studies using other hyperspectral, airborne, and geostationary sensors*** | | | | | | | | | | | | |
| 2009 | Europe | North Sea | SEVIRI MSG | 6S, SOS | TSS | < 100 | NLR | VIS0.6 | 0.79 | - | 63 | (Neukermans *et al.* 2009) |
| 2008 | UK | Barton Broad | CASI-2 | DOS | PC | ~6–158 | LT-LR | *L*710/*L*620 | 0.95 | 19.9 | 13 | (Hunter *et al.* 2008) |
| | | | | | Chl *a* | ~4–63 | LT-LR | *R*710/*R*670 | 0.96 | 18.3 | 13 | |
| 2008 | Spain, Netherlands | 64 freshwater lakes/reservoirs | Spec. | NA | PC | ~0–640 | SA | *R*710/*R*620 | 0.92 | 47.5 $mg.m^{-3}$ | 352 | (Ruiz-Verdú *et al.* 2008) |
| | | | | | PC | ~0–640 | LR | 0.5(*R*600+*R*648)–*R*624 | 0.21 | 135.5 $mg.m^{-3}$ | 352 | |
| | | | | | PC | ~0–640 | LR | *R*650/*R*625 | 0.46 | 119.7 $mg.m^{-3}$ | 352 | |
| 2007 | Italy | Lake Guarda | Hyperion | MODTRAN | Chl *a* | 1.30–2.16 | Analytical | MIP | 0.59 | 20 | 8 | (Giardino *et al.* 2007) |
| | | | | | Turb | 0.95–2.13 | Analytical | MIP | 0.57 | 31 | 7 | |
| 2006 | China | Lake Tai | Spec. | NA | Chl *a* | 20–190 | NLR | *R*719/*R*667 | 0.87 | - | 28 | (Jiao *et al.* 2006) |
| 2006 | US | 15 Minnesota Lakes | Spec. | NA | Chl *a* | 1.8–397 | NLR | *R*700/*R*670 | 0.99 | - | 15 | (Menken *et al.* 2006) |
| 2006 | US | Aquaculture ponds | Spec. | NA | Chl *a* | 107–3078 | LR | (*R*740/*R*710)–(*R*740/*R*650) | 0.78 | 319 $mg.l^{-3}$ | ~64 | (Zimba and Gitelson 2006) |
| 2005 | UK | Tamar Estuary | Spec. | NA | $a_{CDOM}$ | 0.1–1.9 | NLR | *R*400/*R*600 | 0.89 | - | ~43 | (Doxaran *et al.* 2005) |
| 2004 | Finland | Gulf of Finland | Hyperion; ALI | MODTRAN 4; ELM | Chl *a* | 1–1024 | SAM; BOM | - | - | - | - | (Kutser 2004) |
| 2004 | Germany | Lake Constance | CHRIS | RTM | Chl *a* | 1.4–4.4 | Analytical | MIP | - | - | 17 | (Miksa *et al.* 2004) |
| | | | | | TSS | 1.1–2.6 | Analytical | MIP | - | - | 17 | |
| | | | | | $a_{CDOM}$ | 0.13–0.30 | Analytical | MIP | - | - | 17 | |
| 2003 | Australia | Moreton Bay | Hyperion | MODTRAN | Chl *a* | 1.0–19.9 | Analytical | MIP | - | - | - | (Brando and Dekker 2003) |
| | | | | | $a_{CDOM}$ | 0.13–0.75 | Analytical | MIP | - | - | - | |
| | | | | | TSS | 3.4–46.3 | Analytical | MIP | - | - | - | |
| 2002 | France | Gironde Estuary | Spec. | NA | TSS | 13–985 | Poly(3rd) | *R*850/*R*550 | 0.97 | - | 34 | (Doxaran *et al.* 2002) |
| 2000 | Scotland | Clyde Sea | Spec. | NA | $a_{CDOM}$ | ~0.1–1.5 | LR | *R*670/*R*412 | 0.99 | - | 8 | (Bowers *et al.* 2000) |
| 1999 | Netherlands | Lakes, rivers and estuaries | Spec. | NA | Chl *a* | 3–185 | SA | *R*704/*R*672 | 0.95 | 3 $mg.m^{-3}$ | 114 | (Gons 1999) |
| 1998 | US | Nebraska Sand Hills Lakes | Spec. | ELM | Chl *a* | 1–171 | MLR | d*R*429+d*R*695+(d*R*429*d*R*695) | 0.5 | - | 19 | (Fraser 1998) |
| | | | | | Turb | 1–82 | MLR | d*R*429+d*R*628+d695 | 0.69 | - | 30 | |
| 1998 | US | Carter Lake | Spec. | NA | Chl *a* | 20–280 | LR | $RLH_{670-850}$ | 0.86 | ±5.3 $mg.m^{-3}$ | 35 | (Schalles *et al.* 1998) |
| | | | | | Chl *a* | 21–280 | LR | $SUM_{670-850}$ | 0.87 | ±5.3 $mg.m^{-4}$ | 36 | |

| Year | *Country* | *Study area* | *Data type*† | *Atmos. corr.* | *WQPs*‡ | *Data range*§ | *Statistical technique* | *Bands/algorithm*¶ | $r^2$ | *RMSE* \| *(%)* | *N* | *Reference* |
|---|---|---|---|---|---|---|---|---|---|---|---|---|
| 1994 | US | Tennessee Reservoirs | AMMS | None | Chl *a* | 2–79 | LR | *R*700/*R*680 | 0.95 | 2.19 $mg.m^{-3}$ | 29 | (Dierberg and Carriker 1994) |
| | | | | | Chl *a* | 2–79 | LR | $FLH_{663-700}$ | 0.85 | 2.76 $mg.m^{-3}$ | 29 | |
| | | | | | Turb | 1.1–11 | LR | *R*700/*R*680 | 0.88 | 0.93 NTU | 29 | |
| | | | CASI | None | Chl *a* | 1–46 | LR | *L*694/*L*679 | 0.84 | 2 $mg.m^{-3}$ | 34 | |
| | | | | | Chl *a* | 1–46 | LR | $SLH_{665-752}$ | 0.86 | 1.9 $mg.m^{-3}$ | 34 | |
| | | | | | Turb | 1.1–10 | LR | *L*694/*L*679 | 0.77 | 1.0 NTU | 34 | |
| 1994 | Israel | Lake Kinneret | Spec. | NA | Chl *a* | 3.1–7.3 | LR | $SUM_{670-730}$ | 0.84 | 0.69 $mg.m^{-3}$ | 20 | (Gitelson *et al.* 1994) |
| | | | | | Chl *a* | 3.1–7.3 | LR | $FLH_{670-730}$ | >0.73 | 0.77 $mg.m^{-3}$ | 20 | |
| 1993 | Europe | >20 Inland water bodies | Spec. | NA | Chl *a* | 0.1–350 | NLR | *R*700/*R*675 | >0.88 | <2 $mg.m^{-3}$ | >383 | (Gitelson *et al.* 1993) |
| | | | | | TSS | 0.1–66 | NLR | (*R*560–*R*520)/(*R*560+*R*520) | 0.86 | 1.79 $mg.l^{-1}$ | 66 | |
| | | | | | $a_{CDOM}$ | 0.1–12 | NLR | ((*R*480–*R*700/*R*675)–*R*520)/((*R*480+*R*700/*R*675)+*R*520)) | 0.9 | 0.25 $mgC.m^{-3}$ | - | |
| | | | Sl. LS MSS | NA | Chl *a* | 30–150 | MLR | MSS6/MSS4+MSS5+MSS6 | 0.88 | <4.47 $mg.m^{-3}$ | 134 | |
| 1992 | Germany | Laboratory, rivers and lakes | Spec. | NA | Chl a | 5–350 | MLR | *L*705/*L*670 | 0.98 | - | 94 | (Mittenzwey *et al.* 1992) |

† Sl. means simulated.

‡ WQPs = Water Quality Parameters

§ Units for Chl a, PC = $mg.m^{-3}$; TSS, SPIM = $g.m^{-3}$; $a_{CDOM}$ = $m^{-1}$ (at 440 nm unless otherwise stated); $z_{SD}$ = m; TURB = NTU, unless otherwise indicated.

¶ Lx = radiance at wavelength x; Rx =reflectance at wavelength x; DN = Digital Number; Satellite bands are prefixed by the abbreviated sensor's name. Note: coefficients of determination and variables other than spectral bands have not been included. Only algorithms with highest performing correlation coefficients are presented.

| RMSE= Root Mean Square Error. In percentage unless otherwise indicated.

* Total classification accuracy/error.